A thermodynamic study of the effects of membrane composition on the binding affinity of annexin a5

A THESIS SUBMITTED TO THE FACULTY OF
UNIVERSITY OF MINNESOTA
BY

Samantha R. Jaworski

IN PARTIAL FULFILLMENT OF THE REQUIREMENTS
FOR THE DEGREE OF
MASTER OF SCIENCE

Dr. Anne Hinderliter

September 2012

ACKNOWLEDGEMENTS

First, I'd like to thank Dr. Anne Hinderliter for giving me this great opportunity to explore the world of experimental science. I also thank her for her patience and guidance throughout the last two years working in her lab. This work could not have been completed without the help and support of the graduate and undergraduate students working within the Hinderliter lab. The work completed by Jacob Gauer and Kristofer Knutson has been invaluable to the continuation of my project. Moreover, I'd like to thank Michael Fealey, Erika Bladholm, and Jacob Gauer for keeping life both inside and outside research a definite experience. In addition, the help and laughter of Ryan Sisk, Heathere Jacobson, Anne Rice and Ryan Mahling have kept the last year much more interesting. Also, the instructional guidance of the Chemistry Department faculty and staff has been much appreciated. In particular, I'd like to thank Dr. Evans for his patience and expertise with research and instructional questions alike. Lastly, and most importantly, I couldn't have completed any of this work without the unfailing support of my family and close friends.

ABSTRACT

The annexins make up to 2% of all intracellular proteins and have been implicated in a multitude of biological processes; thus, they are a model system for peripheral membrane binding proteins. One member, annexin a5, binds membranes enriched in the acidic phospholipid, phosphatidylserine, and calcium ion. We find by Isothermal Titration Calorimetry (ITC) that annexin a5 binds calcium ions with much higher affinity in the presence of non-cholesterol containing neutral and acidic phospholipid mixtures ((60:40) (POPC:POPS)) relative to solution state (without membrane) calcium ion binding. We hypothesize that the shift to higher affinity calcium ion binding is modulated by the composition of the membrane. We tested this hypothesis by introducing cholesterol, a small, but physiologically significant lipid, to form ternary mixtures of (60:40):5, (60:40):10 and (60:40):20 (POPC:POPS):Chol. Cholesterol enhances the demixing behavior of our binary lipid mixture that is a model of the inner leaflet of the plasma membrane of the eukaryotic cell. Cholesterol and POPS have the weak tendency to form complexes with one another in the background of POPC, which enhances the likelihood of domain formation on the membrane surface. We have shown annexin a5 binds calcium ions with similar affinity in the presence of the ternary mixture containing cholesterol compared to the binary mixture without cholesterol. In contrast, when saturated with calcium ions, annexin a5 binds the ternary membrane system with an enhanced affinity as compared to the binary lipid mixture. This suggests that membrane composition alters the responsiveness of annexin a5 to calcium ion. Moreover, this body of work builds upon, and directly tests our new allosteric transition model of how membrane composition poises membrane associated proteins to respond.

TABLE OF CONTENTS

ABBREVIATIONS

Annexin a5:	Non-human annexin V (rat)
Annexin a4:	Non-human annexin IV
Annexin A5:	Human annexin V
Annexin A2:	Human annexin II
Annexin A6:	Human annexin VI
Annexin A7:	Human annexin VII
POPC:	1-palmitoyl-2-oleoyl-sn-glycero-3-phosphocholine (16:0,18:1PC)
POPS:	1-palmitoyl-2-oleoyl-sn-glycero-3-phospho-L-serine (16:0,18:1PS)
Chol:	(ovine wool, >98%) cholesterol
HEPES:	4-(2-hydroxyethyl)-1-piperazineethanesulfonic acid
βME:	2-mercaptoethanol
PMSF:	phenylmethanesulfonylfluoride
EDTA:	ethylenediaminetetraacetic acid
EGTA:	ethylene glycol-bis(2-aminoethyl-)-N,N, N',N'-tretraacetic acid
BAPTA:	1,2-bis(2-aminophenoxy)ethane-N,N,N',N'-tetraacetic acid
LUV:	large unilamellar vesicle
FCS:	fluorescence correlation spectroscopy
$CaCl_2$:	calcium chloride dihydrate
Milli-Q:	double distilled water
TED:	thermoelectric device
PES:	polyethersulfone

LIST OF TABLES

LIST OF FIGURES

CHAPTER 1: MEMBRANE ORGANIZATION AND THE ANNEXINS

1.1 INTRODUCTION AND BACKGROUND

Biological membranes serve as both a barrier for the cell and a gateway for various messenger molecules and complexes used to carry out necessary physiological functions. The dynamic capacity to transport molecules and complexes through this barrier is based on membrane fluidity and composition. Membrane fluidity is a key regulator of several biological processes and includes the following: endocytosis, exocytosis and apoptosis [1-7]. Membrane size, composition and shape directly impact the ability of proteins, secondary messengers and other signaling complexes to function normally. Cellular membranes are composed of several different lipids that can be either neutral or charged and also have varying degrees of saturation and length. Lipids within membranes include sterols, such as cholesterol (in eukaryotic cells), which modify physical properties, such as permeability and phase behavior.

The Hydrophobic Effect is the major thermodynamic driving force of lipids within an aqueous environment. Lipids are entropically and geometrically driven to form bilayers to minimize contact with water. The acyl chains are oriented towards the inner (non-polar) environment, while the polar head groups interact with the surrounding, aqueous environment. Van der Waals interactions between the hydrocarbon chains of neighboring lipids and hydrogen bonding between certain lipids and their head groups are both stabilizing factors that aid in the Hydrophobic Effect [8-9]. The orientation and configuration of both hydrocarbon chains and polar head groups can introduce various packing arrangements and physical states in lipid mixtures. Below the phase transition temperature of a pure lipid composition (containing one type of lipid), the lipids exist in a gel phase consisting mainly of acyl chains in all trans configurations. This gel phase is more ordered and allows for the elongation of hydrocarbon chains, thus contributing to increasing membrane thickness. As the temperature is increased, the composition transitions through its midpoint or melting temperature in which the lipids are partially in the gel phase and liquid phase [9]. The transition between the gel and fluid phases is dictated by acyl chain interactions; more importantly the transition from all-trans

conformers to more gauche conformers or “kinks” within the hydrocarbon chains [9]. The introduction of kinks and cis-double bonds affect the packing of lipids, which results in a more fluid phase. The addition of lipids of varying chain length, saturation and head groups drastically affects the phase behavior of a pure lipid system [10-13].

A major milestone in the understanding of biological membranes was the fluid mosaic model introduced by Singer and Nicolson [14]. This model described the organization of the membrane as a two-dimensional lipid matrix with integral proteins randomly inserted throughout the membrane bilayer. Cell membranes were highlighted as being fluid, asymmetric, and oriented according to polarity. Non-polar amino acid residues and hydrocarbon chains of lipids are oriented within the bilayer while polar residues and lipid head groups face the aqueous environment [14]. As the field of membrane study expanded, the presence of “clusters” of lipids on the membrane surface were observed [15]. These “clusters” were eventually referred to as lipid domains [2]. The observed presence of lipid domains prompted further study of phase behavior involving various lipid compositions under different conditions (temperature, pressure, pH) [16-21].

Cholesterol is the major sterol found within animal cells and constitutes roughly 20-50% of the lipid mass of the plasma membrane of various animal cells [9, 22]. The presence of cholesterol within the plasma membrane has been directly related to not only membrane fluidity (membrane thickness), but also “lipid rafts” [23-26]. “Lipid rafts” were initially observed as lipid compositions high in cholesterol and glycosphingolipids that were resistant to fractionation experiments using non-ionic detergents [27-30]. Furthermore, the presence of cholesterol within varying model membrane compositions and its effect on its phase behavior has been extensively studied [10-11, 31-33]. Additional fluid states observed within pure-choline lipid systems have been referred to as liquid-ordered and liquid-disordered phases [11-13, 34-35]. The liquid-disordered phase is characterized by less acyl chain order (gauche conformers) at low cholesterol levels (below 10 mole percent), while the liquid-ordered state contains more ordered acyl chains (trans conformers) with increasing cholesterol content (between 10-20 mole percent). Furthermore, above 20 mole percent cholesterol, the liquid-ordered state is

favored, which is significant considering the inner leaflet of the plasma membrane contains roughly 30 mole percent cholesterol. More importantly, these additional fluid states are thought to be more physiologically relevant than that of solely gel to fluid state transitions [22].

Lipid domains are present within the plasma membrane because of differing interactions between lipids and proteins within the bilayer [22, 36]. Lipids have attractive and repulsive interactions with neighboring lipids, proteins and other molecules within the bilayer. These small, preferential interactions between lipids can cause clustering of "like" lipids on the membrane surface [16, 20, 22]. Line tension, which is a result of lipid-lipid interactions, is a driving force of domain formation [37]. The amount of energy necessary to create a boundary between a domain and the surrounding membrane is referred to as line tension [29]. This boundary between a domain and surrounding membrane involves a hydrophobic mismatch of the thicker membrane domains ("rafts") in comparison to the surrounding membrane surface [37-40]. To reduce the line tension at these boundaries, membrane deformation (bending, tilt, and area compression) works to smooth the surface and minimize the hydrophobic surfaces exposed to water at these junctions [37]. The larger the domain, the larger the line tension and the more entropic penalty incurred by merging subsequent domains within the surface. Therefore, it is more thermodynamically and kinetically favorable to have many smaller domains with smaller line tension distributed over the membrane surface [37]. Moreover, studies of model membrane systems suggest that proteins and peptides interact at these boundaries and can reduce line tension [41-42]. Thus, the study of peripheral membrane binding proteins and their interactions with complex lipid systems could lead to a better understanding of both lipid-lipid and protein-lipid interactions and their affects on signal transduction. One such class of proteins known to be involved in protein-lipid interactions and membrane organization is the annexins.

The annexins are a highly conserved, ancient family of proteins that make up 2% of all intracellular proteins within eukaryotes [43-44]. Annexins are Ca^{2+} and phospholipid binding proteins that have been hypothesized to play a role in vesicle transport, endocytosis, exocytosis, apoptosis, signal transduction and protein organization

of lipid membranes [44-46]. However, their exact function remains unclear. All annexins contain a conserved core region consisting of repeating 70 amino acid residues forming four homologous domains, along with a variable NH_2-terminal region [47-48]. These domains of α-helical structure are responsible for calcium dependent binding to phospholipid membranes and are now considered a general membrane binding motif [44, 49]. The variable amino terminal region seen throughout the annexin family is thought to contribute to the functionality of specific annexins [44, 50-51].

Calcium binding to annexins has been observed as an ordered process by means of crystallographic, fluorescent and calorimetric techniques [52-53]. The spatial orientation of annexin is that of an α-helical, curved disk with two principle sides: a more convex side containing Ca^{2+} binding sites that face the membrane surface and a more concave side facing the cytoplasm [44]. These Ca^{2+} binding sites fall between two classes of sites (AB and DE loops) that have been shown to bind one before the other (AB before DE) [47, 52, 54]. More recently, both cooperativity and allostery have been used to describe calcium binding involving various annexins [52-53, 55-56]. Upon binding the phospholipid bilayer, annexins' affinity for calcium is dramatically increased [57-58].

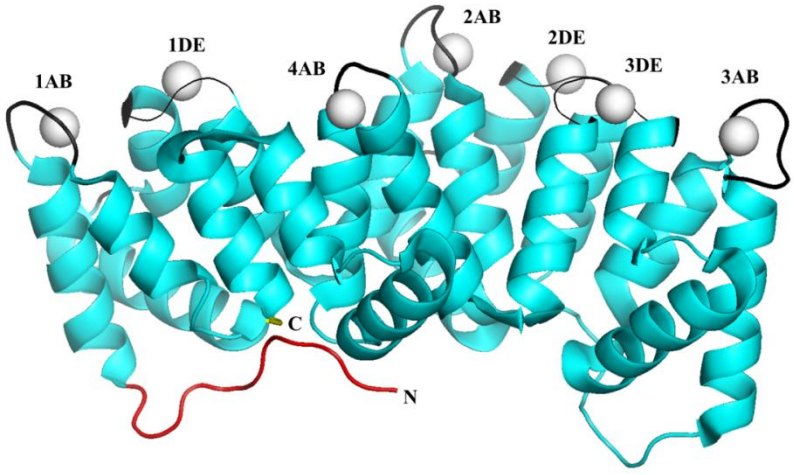

Figure 1.1: The structure of rat annexin a5 [47]. AB and DE binding loops are labeled respectively. The variable N-termini of the annexin is highlighted in red and the C-termini in yellow. PDB file: 2RAN rendered in Pymol Version 1.1.

The ability of annexins to bind the membrane surface allows not only protein-lipid interactions to occur, but in turn affects the underlying organization of lipids on the surface [59]. The formation of trimers by annexin A5 on the membrane surface has been observed using cryo-electron microscopy, X-ray crystallography and chemical cross-linking experiments [60-62]. A two-step model of protein-lipid association has been suggested for annexin A5. First, annexin A5 binds to synthetically modified, phosphatidylserine (PS) molecules in a Ca^{2+} dependent manner and second these PS bound annexin A5 molecules subsequently bind to other annexin A5 molecules either free or bound in solution. Thus, through protein-lipid and weak protein-protein interactions, two-dimensional arrays of annexin A5 were created on the lipid surface [61]. Furthermore, through the use of microscopy and FCS, Ca^{2+}-dependent, membrane binding induces these protein-protein interactions to form annexin a5 assemblies of protein-lipid complexes involving POPS [59]. In addition, further membrane domain organization and annexin self-association has been implicated for 3 of the 12 human annexin isoforms, specifically annexins A2, A6 and A7 [3, 51].

The regulation of intracellular Ca^{2+} levels is extremely sensitive and can induce a variety of biological responses that can vary between membrane repair to apoptosis [50]. The synaptotagmins, SNARES, ferlins and annexins have all been implicated as membrane repair machinery. The least well characterized family of proteins capable of membrane repair is the annexins. The Ca^{2+}-dependent binding of specific negatively charged lipids by different annexins and their relative abundance within the cell, implies they serve important roles as markers of cell distress in addition to actively contributing to membrane repair [50].

In order to effectively study either leaflet of the plasma membrane using model membranes, the phase behavior of lipid compositions is crucial to understanding different interactions (lipid-lipid and protein-lipid) occurring at the membrane surface. The inner leaflet of the plasma membrane is enriched with unsaturated phosphatidylethanolamines, phosphatidylcholine, cholesterol and acidic phospholipids [28, 63]. Therefore, in order to study the binding of an intracellular membrane binding protein, annexin a5, model membranes consisting of neutral and acidic lipids were used. Annexin a5 preferentially

binds phosphatidylserine in the presence of calcium ion, thus mixtures of phosphatidylcholine (POPC) and phosphatidylserine (POPS) were used. Furthermore, the phase behavior of POPC and POPS has been studied. In fact, the clustering of POPS in a background of POPC has been observed [16]. To further model the complexity of the inner leaflet of the plasma membrane, cholesterol was incorporated. In a background of POPC, cholesterol has a preferential interaction toward POPS, thereby enhancing the clustering affect within the model membrane [64-65]. Furthermore, Monte Carlo simulations of experimental lipid-lipid interactions of POPC, POPS and cholesterol were used to visualize the modification of the membrane surface upon introduction of cholesterol [66]. We hypothesized that this enhanced clustering on the membrane surface (domain formation) would further enhance the protein's ability to bind the surface in the presence of calcium ion.

CHAPTER 2: ANNEXIN PURIFICATION, LIPID AND ITC EXPERIMENTAL PREPARATION

2.1 MATERIALS

1-palmitoyl-2-oleoyl-sn-glycero-3-phosphocholine (POPC or 16:0,18:1PC), 1-palmitoyl-2-oleoyl-sn-glycero-3-phospho-L-serine (POPS or 16:0,18:1PS) and cholesterol (ovine wool, >98%) were purchased from Avanti Polar Lipids, Inc. (Birmingham, AL). Potassium chloride (KCl) was Puriss-grade, 3-(N-morpholino)propanesulfonic acid (MOPS) and calcium chloride dihydrate ($CaCl_2$) were Biochemika grade from Fluka Chemical Corp. All buffers used were de-calcified using Chelex-100 ion-exchange resin from Bio-Rad Labs.

2.2 PROTEIN PURIFICATION

Purification of wild-type *Rattus norvegicus* annexin a5 was based on Ca^{2+}-dependent binding to membrane [67]. cDNA encoding rat annexin a5 was kindly provided by H. Sohma (Sapporo Medical University School of Medicine) and was transformed into *Escherichia coli* Bl-21 cells. Overexpression was initiated by the addition of 1 mM isopropyl-ß-D-thiogalactopyranoside at optical densities between 0.4–0.8. After a 5 h induction, cells were harvested by centrifugation and lysed by sonication in 20 mM HEPES, 100 mM KCl, 10 mM $CaCl_2$, 1 mM PMSF and 1 mM βME at pH 7.5. Cellular debris was pelleted by centrifugation at 16,000 rpm for 30 min at 4°C. The pellet, containing annexin a5, was then resuspended in 20 mM MOPS, 100 mM KCl, 20 mM EDTA, 20 mM EGTA and 1 mM βME at pH 7.5 and gently stirred overnight to release annexin. The mixture was then centrifuged and sterile-filtered through a 0.45 µm Millipore PES filter, dialyzed against 20 mM HEPES at pH 8.0, and incubated with 5 mM $MgCl_2$ and benzonuclease (Novagen 90% purity) at a concentration of 10 U for 16 h at 4°C. The protein solution was applied to a pre-equilibrated Q-Sepharose Fast Flow anion exchange column and eluted using a linear gradient from 20 mM to 600 mM NaCl containing 20 mM HEPES and 1 mM βME at pH 8.0. Fractions containing annexin a5

were pooled and filtered using a 0.20 µm Nalgene PES disposable filter unit. Recombinant annexin a5 was then extensively dialyzed in 20 mM MOPS, 100 mM KCl (in excess of 8L) and passed through Chelex-100 resin to remove contaminating Ca^{2+}. Final purity of annexin a5 was >95% as determined by both SDS-PAGE densitometry and a Nanodrop A260/A280 ratio <1. The protein was concentrated using an Amicon Ultra 15 Centrifugal Filter Unit (30,000 MW) from Millipore based on its molecular weight of 35,613 Da. The final concentration was determined using a Nanodrop (Thermo Scientific) at 280 nm (21,050 $M^{-1}cm^{-1}$).

2.3 PREPARATION OF NON-CHOLESTEROL CONTAINING LIPID VESICLES

Large unilamellar vesicles (LUVs) composed of POPC:POPS (60:40, or 80:20, mol/mol) were prepared by aliquotting stock solutions of lipid in chloroform into borosilicate culture tubes using gastight syringes (Hamilton Co., Reno, NV) [68]. Samples were dried to a thin film under a gentle stream of argon and dried for 4 hours under a vacuum of less than 20 mTorr. Samples were then lyophilized by dissolving the lipids in benzene/methanol (19/1, v/v), plunging the samples in liquid nitrogen, and placing them under vacuum (less than 20 mTorr) until the solvent was completely removed (approximately 8 hours). Lipids were hydrated in the dark, to prevent photo degradation, above the gel-fluid phase transition temperature with de-calcified 20 mM MOPS, 100 mM KCl, pH 7.5, under argon. LUVs were prepared by extruding a multilamellar vesicle dispersion through a sandwich of prefilters around a 0.1 µm pore size polycarbonate filter (Avanti Polar Lipids, Inc.) at least 31 times.

2.4 PREPARATION OF CHOLESTEROL CONTAINING LIPID VESICLES

Cholesterol containing LUVs composed of (POPC:POPS):Chol ((60:40):5, (60:40):10, (60:40):20, mol/mol) were prepared by aliquotting stock solutions of lipid in chloroform into a rotary evaporation flask using gastight syringes (Hamilton Co., Reno, NV) [68]. Additional methanol was added to the aliquoted chloroform solution to a final ratio of 4:1 (chloroform: methanol, v/v). The solvent was rapidly evaporated off using a

Buchi R-215 rotary evaporator at 50-60°C. The thin lipid film was placed under a vacuum of less than 20 mTorr for 8 hours. Lipids were hydrated in the dark above the gel-fluid phase transition temperature with de-calcified 20 mM MOPS, 100 mM KCl, pH 7.5, under argon. LUVs were prepared by extruding a multilamellar vesicle dispersion through a sandwich of prefilters around a 0.1 μm pore size polycarbonate filter (Avanti Polar Lipids, Inc.) at least 31 times.

2.5 ISOTHERMAL TITRATION CALORIMETRY

Isothermal titration calorimetry experiments to determine the binding of Ca^{2+} and varying compositions of POPC:POPS and (POPC:POPS):Chol containing lipids to annexin a5 were performed on a TA Instruments Nano Model CSC 5300 ITC at both 15 and 18°C [69]. Titrations were completed at these temperatures due to the nature of the experiments (protein aggregation and flocculation were observed [69], along with laboratory temperature inconsistencies). Both the Ca^{2+} and lipid titrant solutions were prepared in the protein dialysate that was saved after concentrating the protein. This consisted of 20 mM MOPS and 100 mM KCl at pH 7.5 that was passed through Bio-Rad 100 Chelex resin to remove cation impurities and filtered using a 0.2 μm Nalgene PES disposable filter unit. The Ca^{2+} concentrations used in the experiments were verified through the use of BAPTA (Invitrogen/Molecular Probes) and Ca^{2+} electrode (Fisher). The titrant lipid concentration was verified by phosphate assay as described in Kingsley and Feigenson [70-71]. The annexin a5 concentration was directly measured using a Nanodrop (Thermo Scientific) (extinction coefficient of 21,050$M^{-1}cm^{-1}$ at 280 nm) prior to the experiment, but after loading the calorimeter cell. For all experiments, the stir speed was 250 rpm and the interval between injections was 300 s. In addition, all macromolecule-containing, heat of dilution samples and dialysate were thoroughly degassed prior to rinsing and loading both the titration syringe and sample cell.

For experiments in which Ca^{2+} was injected in the presence of both annexin a5 and membrane, a 1.5 mM Ca^{2+} stock (for non-cholesterol experiments) and a 2.5 mM Ca^{2+} stock (for cholesterol experiments) was added to 0.030 mM annexin. For non-cholesterol containing membrane titrations, the injection volume conditions are as

follows: a 1µl injection was used to displace air from the titration syringe followed by 27 × 9 µL injections. For cholesterol containing membrane titrations, the injection volume conditions varied with a 1µl injection used to displace air from the syringe followed by 1 × 3 µL, 1 × 4 µL, 1 × 5 µL, 1 × 6 µL and 33 × 7 µL injections. These titrations were completed at 18°C. The total lipid concentration of 2.0 mM was the same in both the cell and the syringe so that only the enthalpy of binding between annexin a5 and Ca^{2+} in the presence of membrane could be measured. To obtain the enthalpy of binding for Ca^{2+} to annexin a5 in the presence of membrane, raw heats were integrated and the heat of dilution subtracted by injecting the Ca^{2+} and lipid into buffer containing the same concentration of lipid without protein.

For lipid titration experiments, the sample cell was filled with a solution consisting of 0.030 mM annexin a5 and 0.75 mM Ca^{2+}, while the syringe was loaded with 250µL of 35 mM total lipid (LUVs composed of mixtures of POPC:POPS and (POPC:POPS):Chol) and 0.75 mM Ca^{2+}. The use of the same Ca^{2+} concentration in both the cell and the syringe allowed only the enthalpy of membrane binding to be measured. This Ca^{2+} concentration represents 74% saturation of annexin a5 by Ca^{2+}. For both non-cholesterol and cholesterol containing lipid titrations, a 1 µL injection to displace air from the syringe followed by 27 x 9 µL injections resulted in saturated binding profiles. The first two data points were removed due to subsaturation of the protein by lipid (determined using the lipid binding affinity (K_L) for both non-cholesterol and cholesterol containing mixtures). For membrane titrations, raw heats were integrated and the heat of dilution subtracted by injecting the lipid and Ca^{2+} into buffer containing the same concentration of Ca^{2+} without protein. Also, a buffer-buffer titration was conducted as a control ensuring that interfering heats in the buffer were not present.

Between experiments, the sample cell was cleaned by rinsing 5 times with 250 mL of an aqueous solution of 15% Contrad-70 detergent, 15% methanol and 70% Milli-Q water, followed by 5 L of exhaustive rinsing with additional Milli-Q water to remove any contaminating lipids. Titration and injection syringes were rinsed with methanol,

followed by extensive rinsing with de-ionized water to remove any protein or lipid contaminants. Syringes were dried under argon prior to storing.

CHAPTER 3: ISOTHERMAL TITRATION CALORIMETRY AND BINDING THEORY

3.1 ITC BACKGROUND

Binding interactions between macromolecules and their ligands are essential for signal propagation. Muscle contraction, inflammatory response and insulin signaling are all examples of biological signal propagation generated through binding interactions of endogenous ligands and macromolecules [72]. Moreover, a stronger understanding of binding interactions between macromolecules, ions, and other stimuli provide the basis for future medical and pharmaceutical insights in drug development and disease prevention.

Experimentally, the binding of macromolecules, organic and inorganic novel complexes have been studied using fluorescence techniques including binding and immunofluorescence, along with, chemical cross-linking studies [59, 73]. These particular studies normally involve the use of varying probes attached or associated with the complex of interest. Isothermal titration calorimetry (ITC) is an experimental approach that alleviates the use of any additional molecular modifications capable of perturbing the system of interest. Therefore, this technique is extremely powerful when studying sensitive, dynamic systems such as lipids.

Isothermal titration calorimetry uses heat measurement to obtain the thermodynamic enthalpy associated with a binding event. Such binding events can be endothermic (absorb heat from the surroundings) or exothermic (release heat to the surroundings). Calorimeters obtain heat measurements by three different designs: a temperature rise measured in a system of known heat capacity (ΔT), the measured change in power required to maintain a system at a constant temperature (power compensation) or a direct measure of heat flow between the system and large heat sink maintained at a constant temperature (heat flow) [74]. The Nano ITC used for these experiments uses a differential power compensation design. The temperature between the 1.0 mL, 24 K gold sample and reference cells is both controlled and detected by a heater and semiconducting thermoelectric device (TED). The heater maintains a zero temperature

difference between the sample and reference cells. The power required to maintain this zero difference between cells is used as the calorimeter signal, which is collected as a function of time. Thus, a peak in the thermogram is produced when a reaction heat is evolved. Heats evolved are detected on the order of microjoules (μJ). This sensitivity is a powerful means to obtain binding information, yet any slight incompatibility within the system (buffer and pH inconsistencies) will be detected and therefore have deleterious effects. Also, it is important to note that ITC involves using a large amount of material (mM) to obtain a sufficient signal of heat upon binding depending on the system being studied.

For all titrations completed, the sample cell was loaded with macromolecule (annexin a5) while the 250 μL titration syringe, capable of stirring up to 300 rpm, was loaded with ligand (Ca^{2+} and lipid). The titration syringe is equipped with a flattened, slightly twisted paddle tip which physically does the stirring of the solution in the cell. This syringe is finger-tightened into place into the rotating shaft of the burette handle, which is then inserted needle first into the sample cell. The burette handle is then secured by three locking posts after aligning the handle, pressing down and slightly rotating clockwise. Furthermore, volumes of titrant solution between 1-15 μL are controlled and automatically injected by the ITC Run software during a titration.

The determination of the thermodynamic parameters of enthalpy (ΔH), entropy (ΔS) and Gibbs free energy (ΔG) obtained from one experiment is only possible with ITC. In an ITC experiment the overall heat of binding is not measured; rather, it is the heat associated with shifting distributions of states from one set of conditions to another (i.e. changes in protein (macromolecule) and ligand concentrations (bound and free) resulting from each injection). This heat of redistribution is simply the difference between the overall heats associated with the distribution before and after an injection. Therefore, the change in total heat content (ΔQ_i) between the integrated heats of binding at each injection volume are plotted as a function of ligand to macromolecule concentration and used to solve for binding stoichiometry (n), affinity (K) and enthalpy (ΔH). Three available binding models generally used in ITC analysis to solve for these binding parameters include: a single set of independent binding sites [75], multiple sets of

independent binding sites or sequential binding model. The most simplistic model is the Wiseman Isotherm shown below in Equation 1, where the total heat content ($Q_{(i)}$) at each injection is dependent on the bulk ligand (X_t) and macromolecule (M_t) concentrations, the number of binding sites (n), the binding constant (K), and the molar heat of ligand binding (ΔH) [76]. This model is simplistic because an experimental, analytical solution was determined without the use of additional fitting parameters.

$$Q_{(i)} = \frac{nM_t\Delta HV_o}{2}\left(1+\frac{X_t}{nM_t}+\frac{1}{nKM_t}-\sqrt{\left(1+\frac{X_t}{nM_t}+\frac{1}{nKM_t}\right)^2-\frac{4X_t}{nM_t}}\right) \qquad \text{(Eq. 1)}$$

The value of $Q_{(i)}$ is calculated at each injection volume which, again, does not accurately account for the heat released between each injection. To correct for this change in effective volume (V_0) , which is the 0.95 mL volume available for measurement by the instrument, the expression shown in Equation 2 is used [76]. Moreover, the change in volume after each titration injection (V_i or displaced volume) must also be considered and corrected for. The change in heat content (ΔQ_i) from the completion of the *i*-1 injection to the completion of the i^{th} injection is the parameter of interest. This expression describes the integrated heats of binding displayed as a function of ligand to protein ratio in Figures 4.1, 4.2, and 4.3, for example.

$$\Delta Q_{(i)} = Q_{(i)} + \frac{dV_i}{V_o}\left[\frac{Q_{(i)}+Q_{(i-1)}}{2}\right] - Q_{(i-1)} \qquad \text{(Eq. 2)}$$

Moreover, using both the Gibbs free energy relationship, $\Delta G = \Delta H - T\Delta S$, the relationship $\Delta G = RT\ln K_{eq}$ at a constant temperature, along with the molar heat of ligand binding (ΔH) and binding constant (K), the free energy and entropy contributions of binding can be determined.

3.2 PARTITION FUNCTIONS AND UTILITY FOR BINDING

Another approach to modeling binding interactions is through the use of partition functions. A binding partition function (or binding polynomial in this case) is a

mathematical expression accounting for all the possible states a macromolecule or complex can exist [77]. For example, three possible states of annexin a5 are free (unbound) in solution, bound to calcium only, or bound to lipid only. This mathematical expression furthermore uses, in this case, binding constants to account for the distribution of states. To illustrate this, refer to the simplified partition function below (Eq. 3). Q represents all possible protein states relative to the unbound (free) state where [P] is the concentration of free protein, and [PX] is the concentration of bound protein to free ligand [X] [77-78]. Using a simplified portion of a thermodynamic cycle, the binding constant (K_B) can be substituted into the partition function [78].

$$Q = \frac{[P]+[PX]}{[P]} \qquad \text{(Eq. 3)}$$

The probability of the protein being in the free or bound states is determined by the binding constant (K_B) in the binding equilibria below (Eq. 4-5). The larger the binding constant (K_B) or the lower the dissociation constant (K_D), the more likely the protein will exist in the bound state.

$$[P] + [X] \underset{K_B}{\longleftrightarrow} [PX] \qquad \text{(Eq. 4)}$$

$$K_B = \frac{[PX]}{[P][X]} \qquad \text{(Eq. 5)}$$

The relationship between free protein and bound protein can be substituted back into the simplified partition function (binding polynomial) resulting in:

$$Q = 1 + K_B[X] \qquad \text{(Eq. 6)}$$

This expression is dependent on the binding constant (K_B) and the free ligand concentration [X]. Furthermore, the derivative of this binding polynomial with respect to [X] (free ligand), displayed in Equation 7, gives an average number of ligands bound per protein molecule [78].

$$\frac{[X]}{Q} \times \frac{dQ}{d[X]} = \frac{dlnQ}{d\ln[X]} \quad \text{(Eq. 7)}$$

CHAPTER 4: ITC RESULTS OF MEMBRANE TITRATIONS WITHOUT CHOLESTEROL

4.1 ALLOSTERIC TRANSITION MODEL

The binding of annexin a5 with membrane (POPC:POPS) and calcium was examined using ITC. Upon binding the membrane surface, the annexins exhibit an increased affinity for calcium ion in solution [57-58]. Moreover, the binding of some annexins has been observed as cooperative [52-53]. Therefore, to better understand the vague binding mechanism of annexin a5 to its endogenous ligands, ITC was employed.

The data obtained for binding of annexin a5 with calcium ion and membrane (60:40 POPC:POPS) was unable to be properly analyzed using any of the three binding models highlighted previously (Wiseman isotherm, multiple independent sets of binding sites or sequential). Thus, a partition function approach was used to globally fit all data sets. Displayed below in Equation 8 is a semi-grand canonical partition function that represents the distribution of molecular states relative to the ligand-free state:

$$Q = (1 + K_0[Ca^{2+}])^5 + K_L[L]\,(1 + K_{1a}[Ca^{2+}])^2\,(1 + K_{1b}[Ca^{2+}])^3 \qquad \text{(Eq. 8)}$$

The solution state affinity for calcium ion (no membrane present) is represented by $(1 + K_0[Ca^{2+}])^5$. K_0 is the affinity of five, equal and independent Ca^{2+}-binding sites on annexin a5. The affinity of membrane bound annexin a5 for calcium ion is represented by $K_L[L]\,(1 + K_{1a}[Ca^{2+}])^2\,(1 + K_{1b}[Ca^{2+}])^3$. The expression $(1 + K_{1a}[Ca^{2+}])^2$ reflects a high affinity class of two equivalent and independent Ca^{2+}-binding sites with affinity K_{1a}, while $(1 + K_{1b}[Ca^{2+}])^3$ similarly reflects a lower affinity class of three equivalent and independent Ca^{2+}-binding sites with affinity K_{1b}. The term $K_L[L]$ is the probability of being in a membrane-associated conformational state in the absence of Ca^{2+}.

When annexin a5 is titrated with membrane at a fixed calcium ion concentration, the resultant apparent binding constant (K_{app}) becomes a function of calcium ion concentration. The K_{app} binding constant represents the switching of annexin a5 from a Ca^{2+}-bound state in solution to a Ca^{2+}- and membrane-bound state. K_{app} is expressed in terms of the different equilibrium constants describing Ca^{2+} binding (K_0, K_{1a}, and K_{1b}),

the equilibrium constant describing lipid binding in the absence of Ca^{2+} (K_L), and free Ca^{2+} concentration as:

$$K_{app} = K_L (1 + K_{1a}[Ca^{2+}])^2 (1 + K_{1b}[Ca^{2+}])^3 / (1 + K_0[Ca^{2+}])^5 \quad \text{(Eq. 9)}$$

4.2 ITERATIVE DATA ANALYSIS FITTING PROTOCOL

To analyze the annexin a5 binding data, a stepwise approach was taken. This allowed the numerous parameters necessary to describe the system to be determined in a manner that allowed the fewest parameters to float during a given fit. This procedure was as follows:

1. The binding of Ca^{2+} in the absence of membrane was fit first. Note that in the absence of membrane ([L] = 0), the full partition function (Equation 8) simplifies to $Q = (1 + K_0[X])^n$. The results of this fit, n_0, K_0, and ΔH_0, were fixed for all other fitting routines.
2. The binding of Ca^{2+} in the presence of membrane was fit to the full partition function (Equation 8) in a piecewise, iterative fashion. It was assumed that the two trends in the data were due to two sets of Ca^{2+} binding sites, one endothermic with high affinity and one exothermic with low affinity. The expected exothermic heat of binding due to the low affinity sites was fit to determine n_{1b}, K_{1b}, and ΔH_{1b}. The heat contributed from these sites was then subtracted from the total measured signal. The small, yet significant heat of binding from annexin a5 in solution binding Ca^{2+} was accounted for using the fit parameters determined in Step 1. The remaining heat was then fit to the high affinity, endothermic set of sites to determine n_{1a}, K_{1a}, and ΔH_{1a}. An added assumption of conservation of sites ($n_{1a} + n_{1b} = n_0$) further constrained the fits. This process was repeated for several iterations until the reported parameter values converged.
3. The binding of membrane in the presence of Ca^{2+} was fit last. Note that at constant high Ca^{2+} concentration, only two states would dominate (Ca^{2+} saturated annexin a5 in solution or Ca^{2+} saturated annexin a5 on the membrane). This is

also reflected in the overall partition function. For a given Ca^{2+} concentration, it would simplify to $Q = 1 + K_{app}[L]$ where the apparent affinity for membrane, K_{app}, would be constant (Equation 9).

4.3 ITC RESULTS

The raw data measured during the ITC experiments involving membrane (60:40 POPC:POPS) and calcium ion are shown within the top panel of Figures 4.1, 4.2, and 4.3. Each peak represents the heat of binding resulting after an injection. The integrated peak areas are plotted as a function of the ratio between total ligand concentration and total protein concentration within the middle panel of each respective figure. Traditionally, binding isotherms are plotted in a cumulative manner as a function of free ligand [X]. Thus, the bottom panel of each respective figure contains the cumulative heats plotted as a function of increasing free ligand concentration.

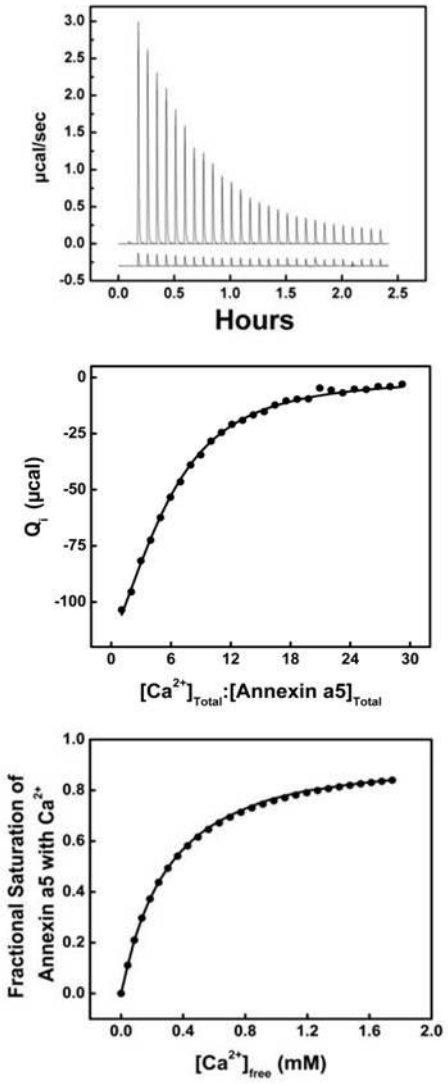

Figure 4.1: Results of the titration of 90 µM annexin a5 with Ca^{2+} at 15°C. *Top*: Raw ITC data. Two titrations are depicted here. The titration above includes annexin a5 under the conditions described, while annexin a5 is absent in the titration below completed under the same experimental conditions (heat of dilution). Middle: Integrated heats of binding as a function of ligand to protein ratio. *Bottom*: Binding isotherm of fractional saturation as a function of free [Ca^{2+}].

4.3.1 CALCIUM ION BINDING BY ANNEXIN A5 IN THE ABSENCE OF MEMBRANE

The titration of annexin a5 with Ca^{2+} in the absence of membrane is shown in Figure 4.1. Here, the measured heat of binding was best fit using a simple binding model

(the Wiseman isotherm) which assumes n_0 independent Ca^{2+} binding sites with equal affinity, K_0, and equal heat of binding, ΔH_0 [79]. These three parameters were found by nonlinear least squares regression to be n_0 = 5.0 ± 0.4, K_0 = (3.1 ± 0.3) x 10^3 M^{-1} ($K_{D,0}$ = 330 ± 40 μM), and ΔH_0 = -2.4 ± 0.2 kcal/mol (Table 1).

TABLE 1: Thermodynamic Parameters for annexin a5 titrations with 60:40 POPC:POPS and Ca^{2+}

	Calcium Ion Binding			Membrane Binding[b]
	Without Membrane	With Membrane, High Affinity	With Membrane, Low Affinity	With Saturating Ca^{2+} Present
N	5.0 ± 0.4	2.0 ± 0.1	3.0 ± 0.1	z = 46.5 ± 0.1
K (M^{-1})	3100 ± 300	410000 ± 120000	5800 ± 100	78000 ± 4000
K_D (μM)	330 ± 40	2.4 ± 1.0	170 ± 10	13 ± 1.0
ΔH (kcal/mol)	-2.4 ± 0.2	3.8 ± 0.2	-13.4 ± 0.4	-17.3 ± 0.1
$T\Delta S$ (kcal/mol)	2.2 ± 0.2	11.2 ± 0.3	-8.5 ± 0.4	-10.9 ± 0.1
ΔG (kcal/mol)	-4.6 ± 0.1	-7.4 ± 0.2	-4.9 ± 0.1	-6.4 ± 0.1

*Reported error represents 95% confidence intervals. The affinity for annexin a5 to bind membrane in the absence of calcium ion was calculated to be K_L = (2.1 ± 0.3) x 10^1 M^{-1} ($K_{D,L}$ = 50 ± 20 mM).

4.3.2 CALCIUM ION BINDING BY ANNEXIN A5 IN THE PRESENCE OF EXCESS MEMBRANE

The titration of annexin a5 with calcium in the presence of membrane is shown in Figure 4.2. The increased complexity in these data is recognizable. The two apparent trends suggest that there is at least two heat producing processes occurring with heats of opposite sign. The measured heat of binding was best fit using a binding model that assumed two sets of linked Ca^{2+} binding sites (see Fitting Protocol section). In short, it was assumed that of the two sets of Ca^{2+} binding sites responsible for these observations:

one consisted of n_{1a} high affinity K_{1a} sites with endothermic heat ΔH_{1a}, and the other with one of n_{1b} low affinity K_{1b} sites and exothermic heat ΔH_{1b}. Furthermore, the total number of Ca^{2+} sites when membrane-associated ($n_{1a} + n_{1b}$) was assumed to be conserved ($n_{1a} + n_{1b} = n_0$), compared to the number of solution Ca^{2+} sites (n_0). Deconvolution of the data was achieved by fitting the individual contributions of each set in an iterative fashion. These results suggest that there were $n_{1a} = 2.0 \pm 0.1$ sites with affinity $K_{1a} = (4.1 \pm 1.2) \times 10^5\ M^{-1}$ ($K_{D,1a} = 2.4 \pm 1.0\ \mu M$) and heat of binding $\Delta H_{1a} = 3.8 \pm 0.2$ kcal/mole (the endothermic, high affinity sites) and $n_{1b} = 3.0 \pm 0.1$ sites with affinity $K_{1b} = (5.8 \pm 0.1) \times 10^3\ M^{-1}$ ($K_{D,1b} = 170 \pm 10\ \mu M$) and heat of binding $\Delta H_{1b} = -13.4 \pm 0.4$ kcal/mol (the exothermic, low affinity sites) (Table 1).

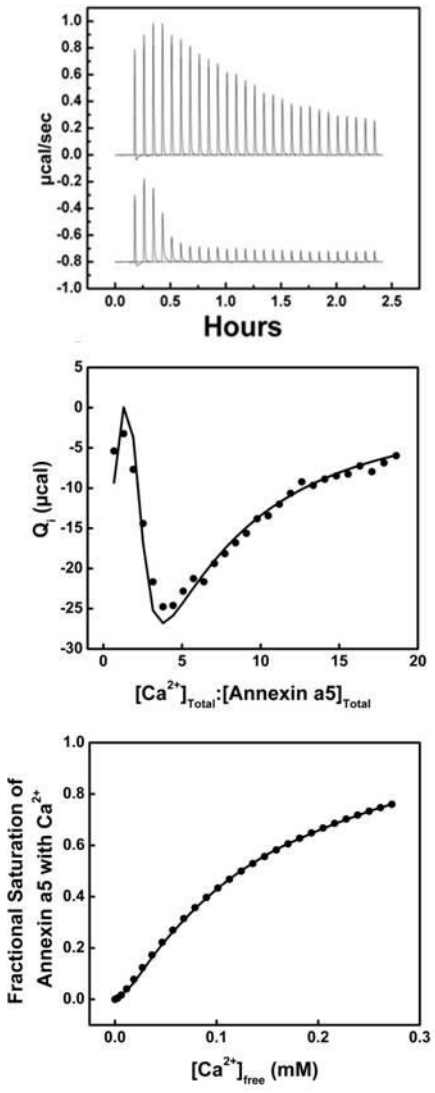

Figure 4.2: Results of the titration of 24 µM annexin a5 with Ca^{2+} in the presence of 2 mM total lipid as LUVs made of a 60:40 mixture of POPC:POPS at 18°C.Top: Raw ITC data. Middle: Integrated heats of binding as a function of ligand to protein ratio. Bottom: Binding isotherm of fractional saturation as a function of free [Ca^{2+}].

4.3.3 MEMBRANE BINDING BY ANNEXIN A5 IN THE PRESENCE OF SATURATING CALCIUM ION

The titration of annexin a5 with phospholipid membranes (LUVs composed of a 60:40 mixture of POPC:POPS) in the presence of Ca^{2+} is shown in Figure 4.3. Note that

only two states dominate at the high Ca^{2+} concentrations present in this titration: annexin a5 in solution, saturated with calcium ion or membrane-associated annexin a5 saturated with Ca^{2+}. The model used described membrane binding as having affinity K_{app} and heat of membrane binding ΔH_{app}. Because differences exist in how stoichiometry of binding is handled when considering binding to a membrane surface versus binding to small ligands, an additional parameter, *z*, was incorporated. This parameter, z, is the average binding stoichiometry of lipids per protein. Annexin a5 binds membrane composed of a 60:40 ratio of neutral to negatively charged lipids in a LUV suspension with an affinity of K_{app} = (7.8 ± 0.4) x 10^4 M^{-1} ($K_{D,app}$ = 13 ± 1.0 μM), a heat of binding of ΔH_{app} = -17.3 ± 0.1 kcal/mol and with an average binding stoichiometry of z = 46.5 ± 0.1 lipids per protein molecule (Table 1).

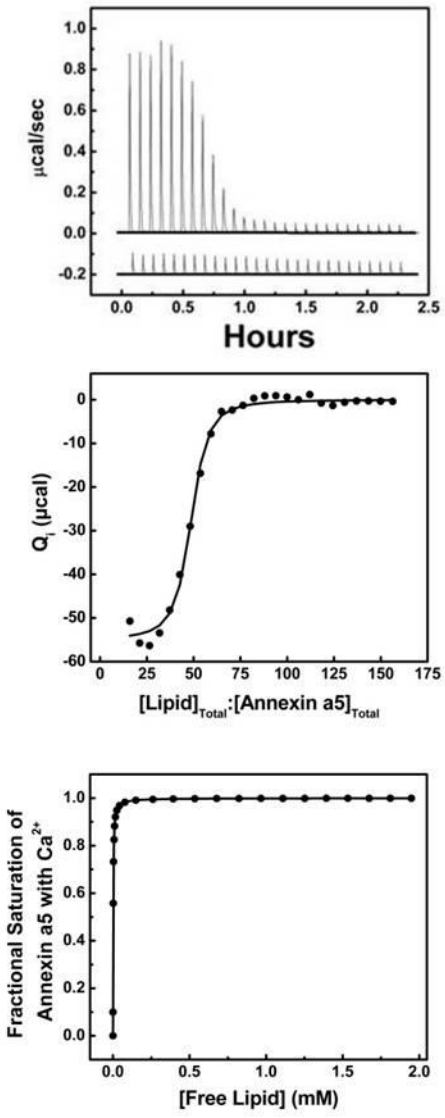

Figure 4.3: Results of the titration of 30 µM annexin a5 with lipid as LUVs made of a 60:40 mixture of POPC:POPS in the presence of 0.75 mM Ca^{2+} at 15°C. *Top*: Raw ITC data. *Middle*: Integrated heats of binding as a function of ligand to protein ratio. *Bottom*: Binding isotherm of fractional saturation as a function of free [Lipid].

4.3.4 MEMBRANE BINDING BY ANNEXIN A5 IN THE ABSENCE OF CALCIUM ION

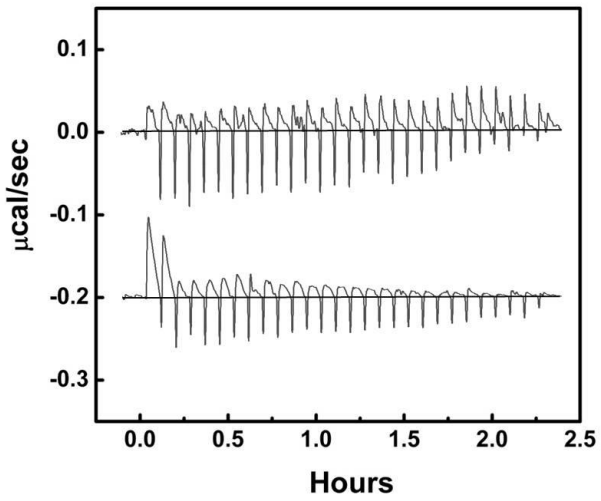

Figure 4.4: Results of the titration of 30 µM annexin a5 with 45 mM total lipid as LUVs made of a 60:40 mixture of POPC:POPS in the absence of Ca^{2+} at 15°C. The raw ITC data is displayed as lipid titrated into annexin a5 (above) and lipid titrated into buffer. The initial abrupt peaks within the heat of dilution data (below) are due to baseline issues resulting from the presence of a bubble within the titration syringe solution during the experiment.

Despite many attempts to measure the heat of membrane binding in the absence of calcium ion (ΔH_L) by ITC, no detectable heats were observed (Figure 4.4). Such results can be interpreted several ways; either the affinity (K_L), or the heat of binding (ΔH_L), or both were insufficient for detection by the calorimeter. Fortunately, the uniquely athermal nature of this binding event provided a means to discriminate between competing binding models. However, by using the mathematical relationship seen in Equation 9, annexin a5's membrane affinity in the absence of Ca^{2+} was calculated to be $K_L = (2.1 \pm 0.3) \times 10^1\ M^{-1}$ ($K_{d,L} = 50 \pm 20$ mM). Because K_{app} is directly proportional to K_L, an accurate determination of K_L is dependent on an accurate determination of K_{app}.

4.4 DISCUSSION

The binding model we present (Section 4.1 and 4.2) is a type of allosteric transition, which is a common theme of biological function [80-81]. We propose Ca^{2+}-stimulated membrane association is a result of differing solution and membrane-associated affinity for calcium. The model is consistent with the cooperative response being due to redistribution of the protein's conformational states. In this case, the redistribution is the switching between two conformational states, one free in solution and one membrane-bound. For such a cooperative response, the ligand-free state of the protein must predominate [80].

Because the membrane-bound state of the protein has a greater affinity for Ca^{2+} than does the solution-state protein, upon Ca^{2+} influx, the membrane bound state binds Ca^{2+} with greater probability. Thus, the membrane-associated (but calcium-ion free) population of protein is depleted upon addition of Ca^{2+}. This state then becomes repopulated by a shift in equilibrium, giving the appearance of an initial plateau in Ca^{2+} binding (due to shifting and replenishing), and then the more abrupt increase in fractional saturation of the high affinity membrane associated calcium binding sites. If the protein was mostly or completely membrane bound, prior to the Ca^{2+} influx, an independent (hyperbolic-shaped) Ca^{2+} binding response would result although binding would occur with the higher affinity of this membrane-associated state. However, if a relatively small population of the protein is membrane-associated (in the initial absence of Ca^{2+}), a cooperative Ca^{2+} binding profile results. Upon Ca^{2+} influx, the protein transitions from an unbound to bound state over a much smaller concentration range of Ca^{2+} than in an independent Ca^{2+} site binding scenario. This cooperative response is possible only if the membrane-bound state of the protein is populated to a relatively low extent in the absence of calcium ligand.

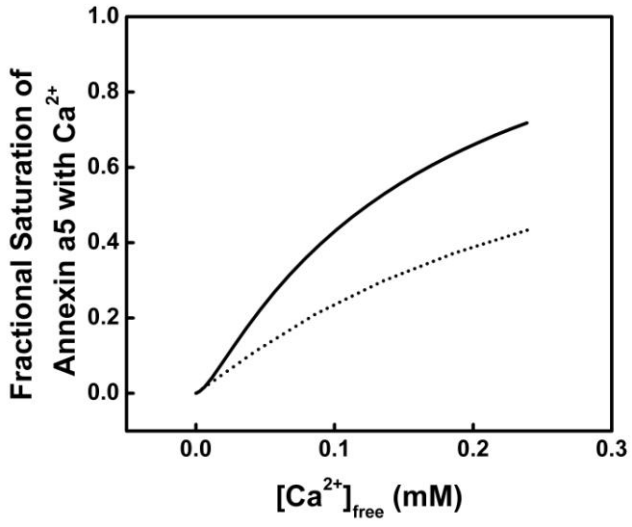

Figure 4.5: Overlay of the binding isotherms for Ca^{2+} binding to annexin a5 in both the solution state (dotted line) and membrane bound (solid line, [L] = 2 mM) states.

To further illustrate the sensitivity of how weak membrane association conveys cooperativity, the binding isotherms of Figures 4.1 and 4.2 (bottom panels) are shown in Figure 4.5. The impact of membrane association becomes apparent as membrane associated annexin a5 is saturated with Ca^{2+} at lower Ca^{2+} concentrations compared to the solution state. The Ca^{2+} saturation exhibits the classic plateau and rise of a cooperative binding process where at a small Ca^{2+} concentration of 100 μM, the fractional saturation of the protein changes from only 20% for solution state protein to 40% when in the presence of membrane. Thus, weak membrane association of annexin a5 greatly enhances its affinity for calcium ion in solution. This cooperative binding response provides a conceptual basis for signal transduction involving annexin-lipid and lipid-lipid interactions on the membrane surface.

CHAPTER 5: ADDITIONAL EXPERIMENTAL RESULTS AND ANALYSIS OF MEMBRANE WITHOUT CHOLESTEROL BINDING IN THE PRESENCE OF CALCIUM ION

To further test our allosteric transition model described in Chapter 4, additional experiments were completed. The experimental variability of K_{app} was evaluated by varying the saturating Ca^{2+} ion concentration for lipid titrations with annexin a5. This variability in turn inversely affected the calculated value K_L (Eq. 9). Moreover, the range of K_L values that captured the K_{app} lipid titrations was found to be limited and highly sensitive. Titrations using a more physiological PS content (roughly 20% within the eukaryotic plasma membrane) were also investigated. Our model was able to reasonably fit the titrations completed with 80:20 POPC:POPS membrane; however, a more robust signal was obtained using the 60:40 POPC:POPS membrane composition. A more defined signal yielded a more dramatic binding profile, which allowed for less error within the analysis. Lastly, a heat partition function was used to recapitulate the calcium binding profile of annexin a5 in the presence of membrane.

5.1 LIPID BINDING AFFINITY CHARACTERIZATION UNDER VARYING CALCIUM ION CONCENTRATIONS

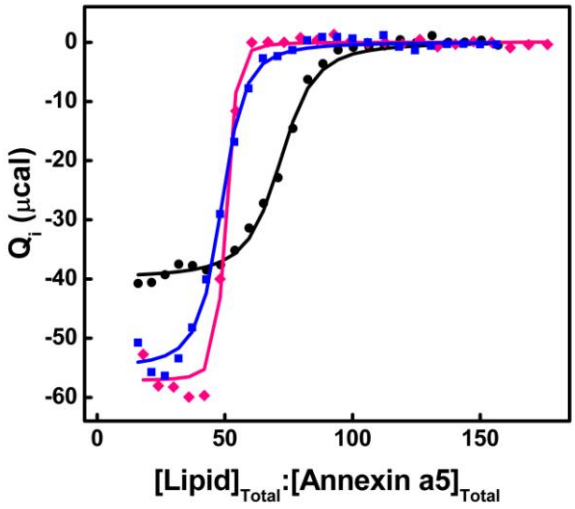

Figure 5.1: Results of the titration of 30 μM annexin a5 with lipid as LUVs made of a 60:40 mixture of POPC:POPS in the presence of 0.5 mM Ca^{2+} (solid black circles), 0.75 mM Ca^{2+} (solid blue squares), and 1 mM Ca^{2+} (solid pink diamonds) at 15°C. Integrated heats of binding are displayed as a function of ligand to protein ratio.

To illustrate the limited window of experimental viability, the K_{app} was evaluated in the presence of 0.50, 0.75 and 1.00 mM calcium ion (Figure 5.1 and Table 2). As annexin a5 becomes increasingly saturated with calcium ion, K_{app} increases. This is a consequence of the term $K_{app} = K_L\ (1 + K_{1a}[Ca^{2+}])^2\ (1 + K_{1b}[Ca^{2+}])^3 / (1 + K_0[Ca^{2+}])^5$ where $[Ca^{2+}]$ is unbound or free in solution. When ITC data is presented as heat versus the total ligand/total protein ratio, the slope is a manifestation of the equilibrium constant. This slope (K_{app}) visibly increases as the protein approaches calcium ion saturation. However, as the system approaches saturation, the experimental sensitivity plummets, as seen in the abrupt change of slope that is characterized by few experimental data points (Figure 5.1). In contrast, with the sub-saturating calcium ion concentration of 0.5 mM, a much more gradual slope is obtained and greater experimental sensitivity is achieved.

However, the 0.5 mM calcium ion concentration does not saturate the system. Therefore, the $(1 + K_{1a}[Ca^{2+}])^2 (1 + K_{1b}[Ca^{2+}])^3 / (1 + K_0[Ca^{2+}])^5$ ratio is not constant throughout the course of the lipid titration. This has a consequence such that, as lipid is added, the membrane-associated affinity for calcium ion is greater than the solution state calcium ion affinity. In this scenario, as lipid is titrated into the suspension of calcium ion and protein, the distribution of lipid-associated and solution state calcium ion binding sites will change, giving rise to a heat profile that has contributions from both lipid binding to calcium-bound annexin a5 and calcium binding to annexin. This complicates the heat profile, as the measured heat is now a compilation of multiple binding events. To retain experimental sensitivity and limit overlap of different ligand binding heats, a compromising calcium ion concentration of 0.75 mM was used. At this concentration, annexin a5 saturation is 74% compared to 77% with 1 mM calcium.

TABLE 2: Additional thermodynamic parameters for annexin a5 titrations with 60:40 POPC:POPS and varying Ca^{2+}

	Calcium Ion Binding			Membrane Binding[b]	
	Without Membrane	With Membrane, High Affinity	With Membrane, Low Affinity	With Saturating Ca^{2+} Present (0.75 mM)	With Saturating Ca^{2+} Present (1 mM)
N	5.0 ± 0.4	2.0 ± 0.1	3.0 ± 0.1	z = 46.5 ± 0.1	z = 47.5 ± 0.1
K (M^{-1})	3100 ± 300	410000 ± 120000	5800 ± 100	78000 ± 4000	790000 ± 185000
K_D (μM)	330 ± 40	2.4 ± 1.0	170 ± 10	13 ± 1.0	1.3 ± 1.0
ΔH (kcal/mol)	-2.4 ± 0.2	3.8 ± 0.2	-13.4 ± 0.4	-17.3 ± 0.1	-18.3 ± 0.1
$T\Delta S$ (kcal/mol)	2.2 ± 0.2	11.2 ± 0.3	-8.5 ± 0.4	-10.9 ± 0.1	-10.6 ± 0.1
ΔG (kcal/mol)	-4.6 ± 0.1	-7.4 ± 0.2	-4.9 ± 0.1	-6.4 ± 0.1	-7.7 ± 0.1

*****Reported error represents 95% confidence intervals. The affinity for annexin a5 to bind membrane in the absence of calcium ion (using the 0.75 mM Ca^{2+} titration K_{app} value) was calculated to be $K_L = (2.1 \pm 0.3) \times 10^1\ M^{-1}$ ($K_{D,L}$ = 50 ± 20 mM). The affinity for annexin a5 to bind membrane in the absence of calcium ion (using the 1 mM Ca^{2+} titration K_{app} value) was calculated to be $K_L = (16 \pm 0.4) \times 10^1\ M^{-1}$ ($K_{D,L}$ = 6 ± 4 mM).

5.2 DETERMINATION OF K_L

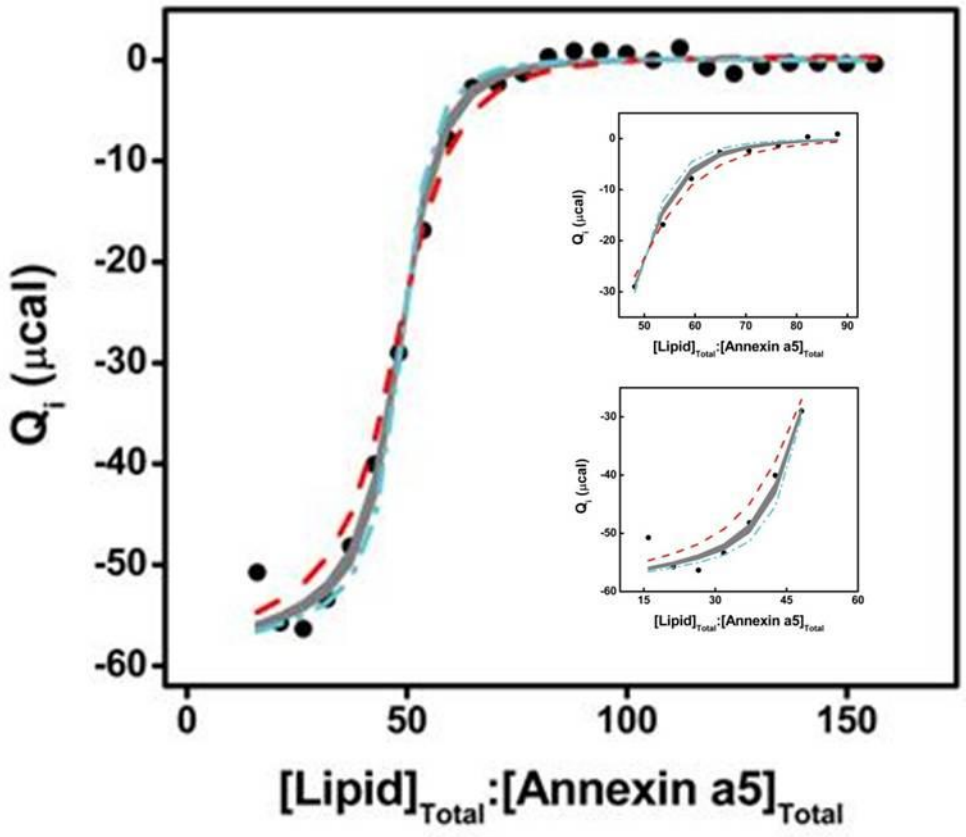

Figure 5.2: Results of the titration of 30 μM annexin a5 with lipid as LUVs made of a 60:40 mixture of POPC:POPS in the presence of 0.75 mM Ca^{2+} (solid black circles). The range of the calculated K_L value with 95% confidence is depicted by the solid grey line. The simulated fits of calculated K_L values of 10 M^{-1} (dashed red line) and 35 M^{-1} (dashed-dot light blue line) are shown to display the narrow experimental window of K_L values that capture the integrated heats of binding. Both inset graphs highlight the difference in fit with varying K_L values (dashed red and dashed-dot light blue lines) in comparison to the 95% confidence interval of the calculated fit which is $K_L = (2.1 \pm 0.3) \times 10^1$ M^{-1}(solid grey line).

K_{app} and K_L are inversely proportional. To thus define K_L, we varied K_L to define the range over which K_{app} described the data. The range over which K_L could vary and thus still globally describe the binding data in the presence of lipid is shown in Figure

5.2. To accurately capture the inflection point of the binding curve (Figure 5.2) in addition to the nuances of the inset regions highlighted, correct calculation of the K_L value within a statistical range is necessary. The sensitivity of the K_L value is illustrated by the two additional K_L values (shown in red and light blue respectively) used to simulate the additional fits shown. The inflection point of the curve is reasonably satisfied by all K_L values shown (including the additional fits). However, the insets clearly emphasize the slight variation of the additional K_L values' fits with respect to the integrated raw data. It is evident that the K_L range that describes the data is limited. Thus, the calculated, relative low affinity of annexin a5 for membrane in the absence of calcium ion using the new allosteric transition model presented accurately describes the data.

5.3 ADDITIONAL DATA COLLECTED UNDER MORE PHYSIOLOGICALLY RELEVANT POPS CONCENTRATIONS

The experiments highlighted previously (Figures 4.1-4.4), were carried out in 40% POPS in a background of 60% POPC. We had determined that annexin a5 generates a heat upon ligating POPS but not POPC. Previous work indicates that annexin a5 and a4 do not have sufficient specificity to redistribute PS in a background of PC [55]. The linearity of K_L with PS content (noted in Figure 8 of reference [55]) is consistent with annexin a5 not remodeling the membrane surface upon binding. Therefore, to maximize experimental sensitivity, the experiments were carried out at a non-physiological POPS content with the assumption that via partition functions, the K_L for physiological PS levels (~20%) could be extrapolated. By maximizing POPS content, less protein was necessary to generate a robust signal which is more amenable to analysis and consequently less calcium ion was required to saturate the system (enabling K_{app} to be defined). To illustrate, the experiments were repeated with 20% POPS in a background of 80% POPC but with increased total lipid concentration to compensate for the reduced mole percent POPS within the 20:80 (POPS:POPC) mixture as compared to the 40:60 (POPS:POPC) mixture; thus, the POPS content is the same at each injection point (Figure 5.3). Upon injecting annexin a5 in the presence of 20:80 (POPS:POPC) with calcium ion, a noticeable difference in the resultant data is evident when compared with data collected in the presence of 40:60 (POPS:POPC). Due to the less pronounced dip in the calcium titration into annexin a5 and 20:80 (POPS:POPC), it is difficult to analyze the overall binding isotherm. While the total POPS concentration was conserved between the 40:60 (POPS:POPC) and 20:80 (POPS:POPC) experiments by varying the total lipid concentration, the 40:60 (POPS:POPC) has both greater signal change and shape to the binding profile. The less discriminating fit of the 20:80 (POPS:POPC) data is evident by the greater error associated with this data as compared to the 40:60 (POPS:POPC) data (Table 3). However, it should be noted that the K_L values overlap as expected with the same POPS content.

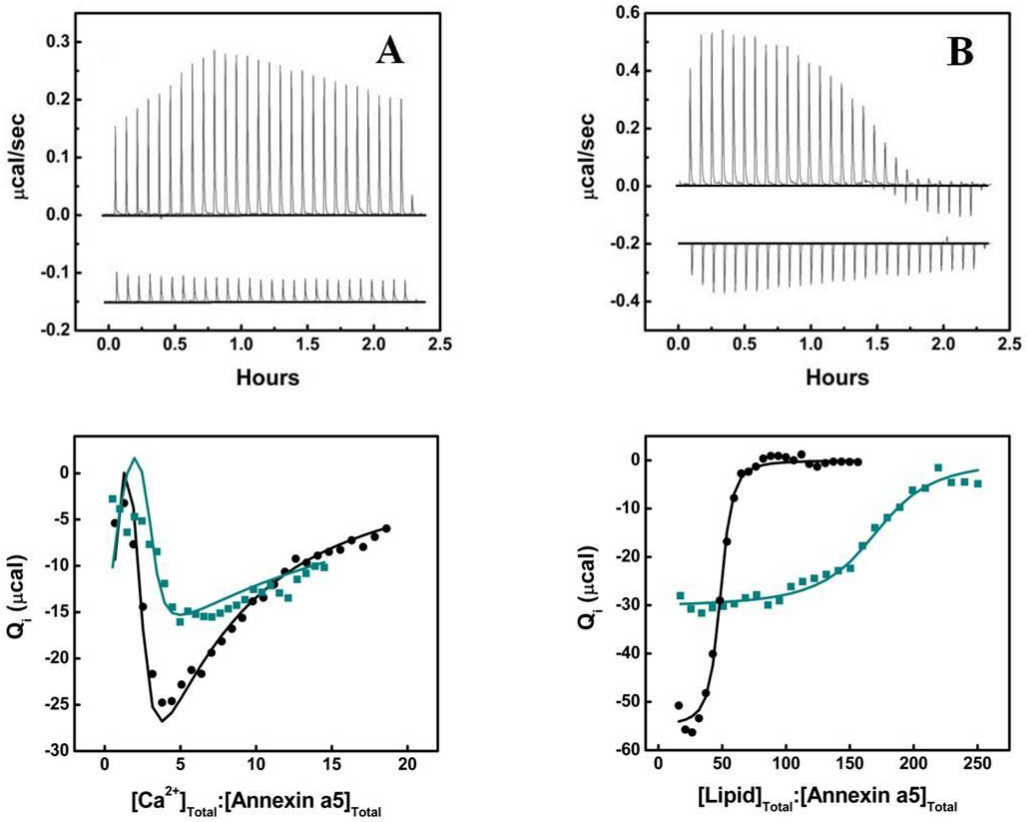

Figure 5.3: (A) Results of the titration of 24 µM annexin a5 with Ca^{2+} in the presence of 2 mM total lipid as LUVs made of a 60:40 mixture of POPC:POPS at 18°C (solid black circles). Results of the titration of 30 µM annexin a5 with Ca^{2+} in the presence of 4 mM total lipid as LUVs made of a 80:20 mixture of POPC:POPS at 18°C (solid cyan squares). *Top*: Raw ITC data from the titration of 30 µM annexin a5 with Ca^{2+} in the presence of 4 mM total lipid made of a mixture of 80:20 POPC:POPS at 18°C. *Bottom*: Integrated heats of binding displayed as a function of ligand to protein ratio of both annexin a5 with Ca^{2+} in the presence of 2 mM total lipid made of a mixture of 60:40 POPC:POPS (solid black circles) and in the presence of 4 mM total lipid made of a mixture of 80:20 POPC:POPS (solid cyan squares).

(B) Results of the titration of 30 µM annexin a5 with lipid as LUVs made of a 60:40 mixture of POPC:POPS in the presence of 0.75 mM Ca^{2+} (solid black circles) at 15°C. Results of the titration of 19 µM annexin a5 with lipid as LUVs made of a 80:20 mixture of POPC:POPS in the presence of 0.75 mM Ca^{2+} (solid cyan squares) at 15°C. *Top*: Raw ITC data from the titration of 19 µM annexin a5 with lipid composed of a mixture of 80:20 POPC:POPS in the presence of 0.75 mM Ca^{2+} at 15°C. *Bottom*: Integrated heats of binding displayed as a function of ligand to protein ratio of both annexin a5 with lipid composed of a 60:40 POPC:POPS mixture (solid black circles) and 80:20 POPC:POPS mixture (solid cyan squares) in the presence of 0.75 mM Ca^{2+}.

TABLE 3: Thermodynamic parameters for annexin a5 titrations with 80:20 POPC:POPS and Ca^{2+}

	Calcium Ion Binding		Membrane Binding
	With Membrane, High Affinity	With Membrane, Low Affinity	With Saturating Ca^{2+} Present (0.75 mM)
N	3.0 ± 0.1	10 ± 0.7	51.8 ± 0.1
K (M^{-1})	500000 ± 193000	970 ± 70	62000 ± 2000
K_D (μM)	2.0 ± 1.0	1000 ± 80	16 ± 0.5
ΔH (kcal/mol)	1.5 ± 0.1	-7.3 ± 0.8	-34.8 ± 0.1
$T\Delta S$ (kcal/mol)	9.1 ± 0.2	-3.3 ± 0.8	-28.5 ± 0.1
ΔG (kcal/mol)	-7.6 ± 0.2	-4.0 ± 0.1	-6.3 ± 0.1

*Reported error represents 95% confidence intervals. The affinity for annexin a5 to bind membrane in the absence of calcium ion was calculated to be $K_L = (1.6 \pm 0.3) \times 10^1\ M^{-1}$ ($K_{D,L} = 60 \pm 30$ mM).

5.4 HEAT PARTITION FUNCTION

As a final test of our fitted values of enthalpy (ΔH), association constants (K) and number of binding sites (n) for the thermodynamic cycle, the fractional distribution of states at each point in the experiments were multiplied by the associated heats and overlaid with the data (Figure 5.4).

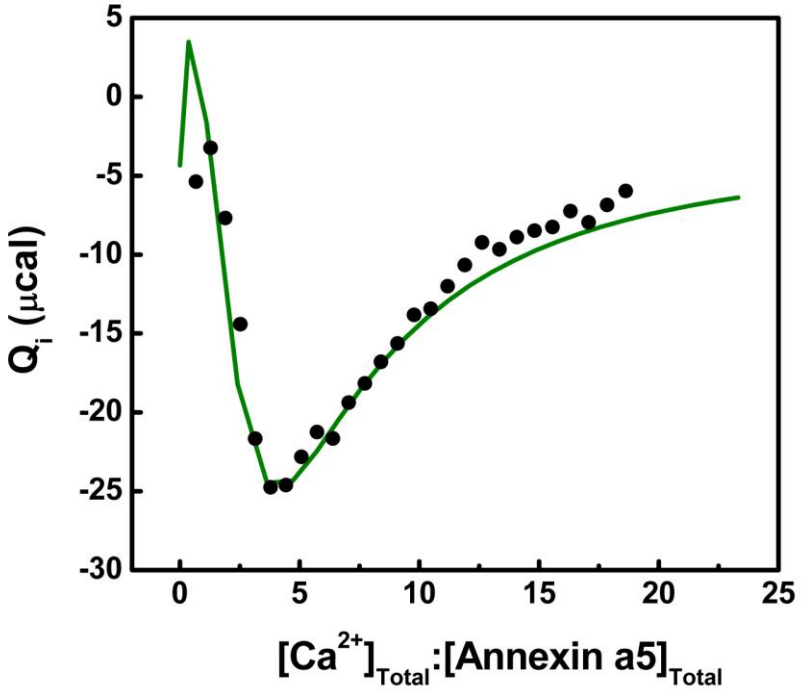

Figure 5.4: Calculation of heats through the use of partition functions and the fit parameters of enthalpy, equilibrium constants and binding stoichiometries simulating the integrated heats obtained by the titration depicted in Figure 4.3. The thermodynamic fit parameters including the enthalpies (ΔH), association constants (*K*), and number of binding sites (n_{1a}, $n_{1b,}$ and n_o) were multiplied by the corresponding fractional distribution of states at each injection of the titration. These total heats for each state were then summed and the change in total heat between each point in the titration was determined. The integrated heats of binding as a function of ligand to protein ratio from Figure 4.3 (solid black circles) are overlaid with the total heats simulated by the heat partition function (green line).

CHAPTER 6: CHOLESTEROL CONTAINING MEMBRANE BINDING STUDIES

6.1 CHOLESTEROL ITC RESULTS

Cholesterol is an important physiologic lipid that has been shown to have dramatic effects on phase behavior and other physical properties of membranes [10-11, 31-33]. More specifically, cholesterol incorporation within the binary composition of POPC and POPS has been shown to induce "clustering" of POPS and cholesterol, forming lipid domains [64-66]. This clustering event or domain formation is a means of biological communication and signal propagation. Moreover, protein-protein interactions at the membrane surface by annexin a5 were hypothesized to further enhance protein-lipid interactions. With these increased interactions between annexin a5 and "clustered" POPS domains, we hypothesized there would be an enhancement of the protein's affinity for this surface in the presence of calcium.

To investigate the affects of membrane composition and membrane organization on the binding affinity of annexin a5 in both the presence and absence of calcium ion, we introduced cholesterol into POPC:POPS vesicles. When considering a ternary phase diagram, allowing two of the three component fractions to remain the same results in a less complicated (two-dimensional) diagram. This more simplified diagram restricts the degrees of freedom allowed for a given composition, thus enabling the study of one changing variable in comparison to multiple variables. This is the basis for the total mole fraction of POPC:POPS (60:40 or 100%) remaining constant within the vesicles prepared. Nonetheless, the additional 5, 10 and 20 mole percents cholesterol incorporated into the vesicles decreased the total phospholipid content (both POPC and POPS). For example, the addition of 20 mole percent cholesterol ((60:40):20) into a 1 mM total lipid concentration results in a decrease in total phospholipid from 100 mole percent to 80 mole percent. Thus, the individual POPC and POPS mole fractions are reduced in the presence of cholesterol (as shown by the calculation below).

$0.80 \times (0.6) = 0.48$ mole percent POPC

$0.80 \times (0.4) = 0.32$ mole percent POPS (Eq. 10)

The decreased total phospholipid content (0.80) is multiplied by the original POPC and POPS phospholipid ratios (0.6 and 0.4) respectively. Therefore, both the POPC and POPS content are reduced in the presence of 20 mole percent cholesterol. The modified POPC and POPS content as a function of increasing cholesterol content in 2 mM total lipid concentrations is illustrated in Table 4.

TABLE 4: Calculated change in POPC and POPS content with cholesterol addition

	Membrane Composition (2mM total lipid)			
Phospholipid Content	60:40 POPC:POPS	(60:40):5 (POPC:POPS) :Chol	(60:40):10 (POPC:POPS) :Chol	(60:40):20 (POPC:POPS) :Chol
POPC (mol %)	0.60	0.57	0.54	0.48
POPS (mol %)	0.40	0.38	0.36	0.32

ITC calcium and lipid titration experiments were conducted under similar conditions as those previously mentioned for non-cholesterol containing membrane experiments (refer to Chapter 2). The same iterative approach to fitting non-cholesterol containing membrane data was used for all cholesterol experiments. However, major differences were observed for the calcium titrations in the presence of membrane. The amount of total calcium needed to saturate the system increased by roughly 1 mM total Ca^{2+}. Furthermore, using an identical analysis approach, the total number of calcium binding sites in the presence of cholesterol-containing membrane could no longer be constrained to $n_0 = 5$, that of solution state annexin a5 binding.

Similar calcium binding profiles in the presence of cholesterol containing membrane, those consistent with two classes of high and low affinity binding sites, were observed (Figures 6.1, 6.2, and 6.3). The characteristic "U" shape displaying the two heat evolving processes occurring is consistent with that seen in the presence of non-cholesterol containing membrane. The most dramatic comparison of calcium binding profiles is seen in Figure 6.4. The overall change in total heat between varying lipid compositions is significantly different and is manifested in the binding affinities of both classes of sites. Cholesterol-containing membrane compositions further modified annexin a5's binding affinity in the presence of calcium as compared to both the solution state (without membrane) and the non-cholesterol containing membrane associated state (Tables 5, 6, and 7).

6.1.1 CALCIUM ION BINDING BY ANNEXIN A5 IN THE PRESENCE OF 5 MOLE PERCENT CHOLESTEROL CONTAINING MEMBRANE

The titration of annexin a5 with calcium in the presence of the (60:40):5 (POPC:POPS):Chol mixture is shown in Figure 6.1. The two similar trends again suggest two heat producing processes occurring with heats of opposite sign. The total number of Ca^{2+} sites when membrane-associated could no longer be assumed to be conserved ($n_{1a} + n_{1b} = n_0$). The change in number of both high and low affinity binding sites is significant. These results suggest that there are $n_{1a} = 1.0 \pm 0.1$ sites with affinity $K_{1a} = (11 \pm 1.3) \times 10^5\ M^{-1}$ ($K_{D,1a} = 0.9 \pm 0.1$ µM) and heat of binding $\Delta H_{1a} = 3.3 \pm 0.1$ kcal/mol (the endothermic, high affinity sites) and $n_{1b} = 5.0 \pm 0.2$ sites with affinity $K_{1b} = (13 \pm 0.7) \times 10^3\ M^{-1}$ ($K_{D,1b} = 74 \pm 4.0$ µM) and heat of binding $\Delta H_{1b} = -5.1 \pm 0.2$ kcal/mol (the exothermic, low affinity sites) (Table 5).

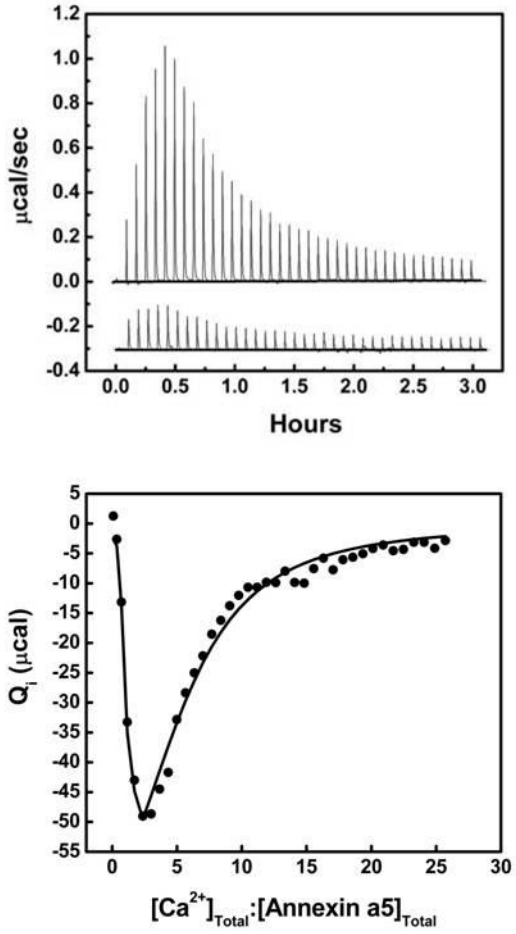

Figure 6.1: Results of the titration of 30 µM annexin a5 with Ca^{2+} in the presence of 1.8 mM total lipid as LUVs made of a (60:40):5 mixture of (POPC:POPS):Chol at 18°C. *Top*: Raw ITC data. *Bottom*: Integrated heats of binding as a function of ligand to protein ratio.

TABLE 5: Thermodynamic parameters of calcium binding of annexin a5 in the presence of (60:40):5 (POPC:POPS):Chol

	Calcium Ion Binding		
	Without Membrane	With (60:40):5 (PC:PS):Chol Membrane, High Affinity	With (60:40):5 (PC:PS):Chol Membrane, Low Affinity
N	5.0 ± 0.4	1.0 ± 0.1	5.0 ± 0.2
K (M^{-1})	3100 ± 300	1100000 ± 130000	13000 ± 700
K_D (μM)	330 ± 40	0.9 ± 0.1	74 ± 4.0
ΔH (kcal/mol)	-2.4 ± 0.2	3.3 ± 0.1	-5.1 ± 0.2
$T\Delta S$ (kcal/mol)	2.2 ± 0.2	11.3 ± 0.1	0.4 ± 0.2
ΔG (kcal/mol)	-4.6 ± 0.1	-8.0 ± 0.1	-5.5 ± 0.1

*Reported error represents 95% confidence intervals. Calcium ion binding is compared to that of solution state binding (without membrane).

6.1.2 CALCIUM ION BINDING BY ANNEXIN A5 IN THE PRESENCE OF 10 MOLE PERCENT CHOLESTEROL CONTAINING MEMBRANE

The titration of annexin a5 with calcium in the presence of the (60:40):10 (POPC:POPS):Chol mixture is shown in Figure 6.2. Two heat producing processes occurring with heats of opposite sign are observed again. Moreover, the total number of Ca^{2+} sites when membrane-associated could no longer be assumed to be conserved, as observed before upon the addition of 5 mole percent cholesterol. These results suggest that there are n_{1a} = 1.0 ± 0.1 sites with affinity K_{1a} = (14 ± 3.7) x 10^5 M^{-1} ($K_{D,1a}$ = 0.7 ± 0.2 μM) and heat of binding ΔH_{1a} = 2.8 ± 0.2 kcal/mol (the endothermic, high affinity sites) and n_{1b} = 5.0 ± 0.2 sites with affinity K_{1b} = (12 ± 0.5) x 10^3 M^{-1} ($K_{D,1b}$ = 84 ± 4.0 μM) and heat of binding ΔH_{1b} = -5.0 ± 0.2 kcal/mol (the exothermic, low affinity sites) (Table 6). These parameters are almost identical to those described in Table 5 for calcium binding in the presence of 5 mole percent cholesterol.

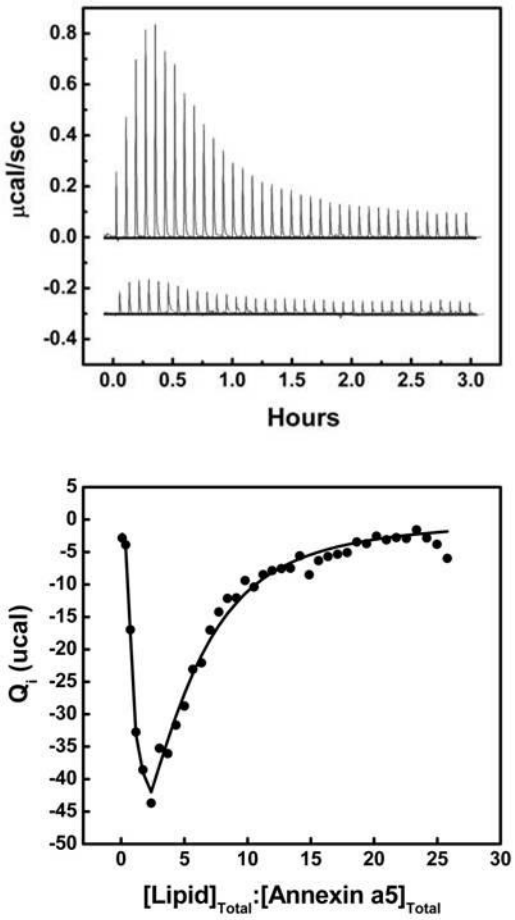

Figure 6.2: Results of the titration of 30 µM annexin a5 with Ca^{2+} in the presence of 2.1 mM total lipid as LUVs made of a (60:40):10 mixture of (POPC:POPS):Chol at 18°C. *Top*: Raw ITC data. *Bottom*: Integrated heats of binding as a function of ligand to protein ratio.

TABLE 6: Thermodynamic parameters of calcium binding of annexin a5 in the presence of (60:40):10 (POPC:POPS):Chol

	Calcium Ion Binding		
	Without Membrane	With (60:40):10 (PC:PS):Chol Membrane, High Affinity	With (60:40):10 (PC:PS):Chol Membrane, Low Affinity
N	5.0 ± 0.4	1.0 ± 0.1	5.0 ± 0.2
K (M^{-1})	3100 ± 300	1400000 ± 370000	12000 ± 500
K_D (μM)	330 ± 40	0.7 ± 0.2	84 ± 4.0
ΔH (kcal/mol)	-2.4 ± 0.2	2.8 ± 0.2	-5.0 ± 0.2
$T\Delta S$ (kcal/mol)	2.2 ± 0.2	11.0 ± 0.3	-0.4 ± 0.2
ΔG (kcal/mol)	-4.6 ± 0.1	-8.2 ± 0.2	-5.4 ± 0.1

*Reported error represents 95% confidence intervals. Calcium ion binding is compared to that of solution state binding (without membrane).

6.1.3 CALCIUM ION BINDING BY ANNEXIN A5 IN THE PRESENCE OF 20 MOLE PERCENT CHOLESTEROL CONTAINING MEMBRANE

The titration of annexin a5 with calcium in the presence of the (60:40):20 (POPC:POPS):Chol mixture is shown in Figure 6.3. The two heat producing processes occurring here were much less dramatic than both 5 and 10 mole percent integrated heats of binding. Although, the total number of Ca^{2+} sites was doubled in comparison to both 5 and 10 mole percent containing cholesterol titrations. These results suggest that there are n_{1a} = 1.0 ± 0.1 sites with affinity K_{1a} = (11 ± 1.8) x 10^5 M^{-1} ($K_{D,1a}$ = 0.9 ± 0.2 μM) and heat of binding ΔH_{1a} = 1.4 ± 0.1 kcal/mol (the endothermic, high affinity sites) and n_{1b} = 12.0 ± 0.3 sites with affinity K_{1b} = (11 ± 1.2) x 10^3 M^{-1} ($K_{D,1b}$ = 94 ± 11 μM) and heat of binding ΔH_{1b} = -2.1 ± 0.1 kcal/mol (the exothermic, low affinity sites) (Table 7).

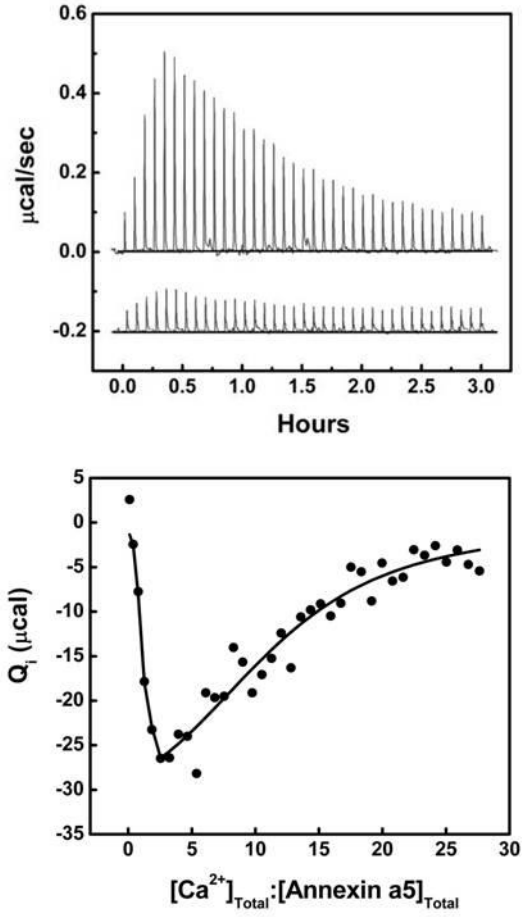

Figure 6.3: Results of the titration of 28 µM annexin a5 with Ca^{2+} in the presence of 2 mM total lipid as LUVs made of a (60:40):20 mixture of (POPC:POPS):Chol at 18°C. *Top*: Raw ITC data. *Bottom*: Integrated heats of binding as a function of ligand to protein ratio.

TABLE 7: Thermodynamic parameters of calcium binding of annexin a5 in the presence of (60:40):20 (POPC:POPS):Chol

	Calcium Ion Binding		
	Without Membrane	With (60:40):20 (PC:PS):Chol Membrane, High Affinity	With (60:40):20 (PC:PS):Chol Membrane, Low Affinity
N	5.0 ± 0.4	1.0 ± 0.1	12.0 ± 0.3
K (M^{-1})	3100 ± 300	1100000 ± 180000	11000 ± 1200
K_D (μM)	330 ± 40	0.9 ± 0.2	94 ± 11
ΔH (kcal/mol)	-2.4 ± 0.2	1.4 ± 0.1	-2.1 ± 0.1
$T\Delta S$ (kcal/mol)	2.2 ± 0.2	9.4 ± 0.1	3.2 ± 0.1
ΔG (kcal/mol)	-4.6 ± 0.1	-8.0 ± 0.1	-5.3 ± 0.1

*Reported error represents 95% confidence intervals. Calcium ion binding is compared to that of solution state binding (without membrane).

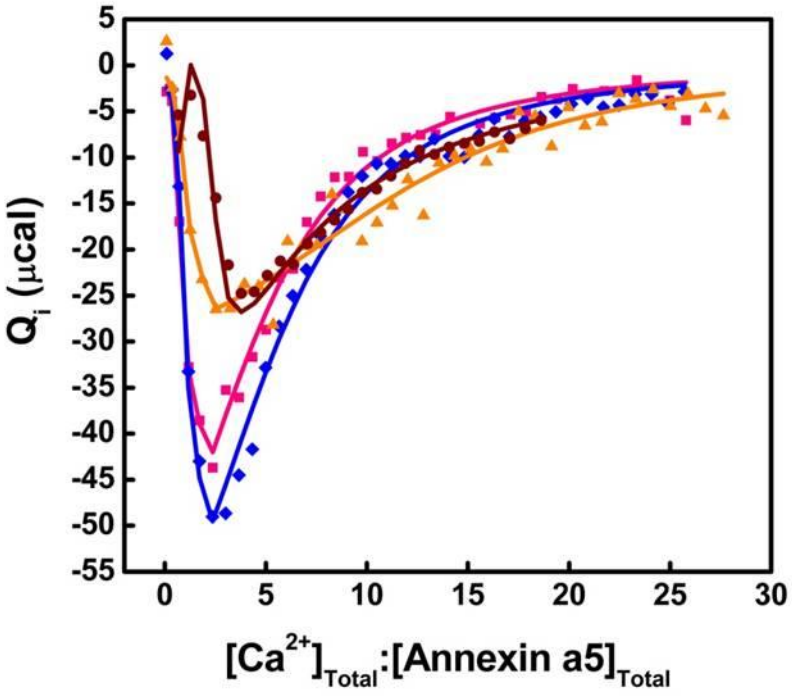

Figure 6.4: Results of multiple titrations of 30 µM annexin a5 with Ca^{2+} in the presence of 2 mM total lipid as LUVs made of mixtures of 60:40 POPC:POPS (maroon circles), (60:40):5 (POPC:POPS):Chol (blue diamonds), (60:40):10 (POPC:POPS):Chol (pink squares) and (60:40):20 (POPC:POPS):Chol (orange triangles) at 18°C. The integrated heats of binding as a function of ligand to protein ratio are shown overlaid.

The overlaid Ca^{2+} titrations in the presence of non-cholesterol and cholesterol containing membrane are shown in Figure 6.4. The differences in binding profiles in the presence of varying membrane compositions are readily apparent. Overall, this data suggests that an increase in cholesterol content possibly induces calcium binding sites within the protein or the presence of specific membrane compositions elucidates varying binding responses of the protein in the presence of calcium ion.

6.1.4 CHOLESTEROL CONTAINING MEMBRANE BINDING BY ANNEXIN A5 IN THE PRESENCE OF SATURATING CALCIUM ION

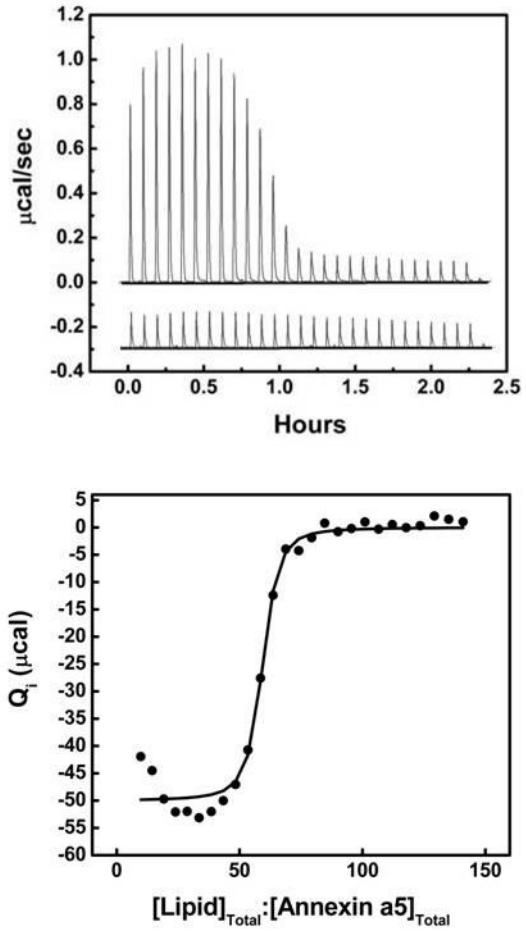

Figure 6.5: Results of the titration of 29 µM annexin a5 with lipid as LUVs made of a (60:40):5 mixture of (POPC:POPS):Chol in the presence of 0.75 mM Ca^{2+} at 15°C. Top: Raw ITC data. Bottom: Integrated heats of binding as a function of ligand to protein ratio.

The titration of annexin a5 with phospholipid membranes (LUVs composed of (60:40):5 and (60:40):10 mixtures of (POPC:POPS):Chol) in the presence of Ca^{2+} are shown in Figures 6.5 and 6.6. Membrane binding in the presence of saturating calcium ion is still described as the affinity (K_{app}). Annexin a5 binds membrane composed of a (60:40):5 ratio of (POPC:POPS):Chol in a LUV suspension with an affinity of K_{app} = (1.9

± 0.6) x 10^5 M^{-1} ($K_{D,app}$ = 5.2 ± 2.0 μM), a heat of binding of ΔH_{app} = -20.0 ± 0.1 kcal/mol and with an average binding stoichiometry of z = 57.0 ± 0.4 lipids per protein molecule (Table 8). Annexin a5 binds membrane composed of a (60:40):10 ratio of (POPC:POPS):Chol in a LUV suspension with an affinity of K_{app} = (2.4 ± 0.7) x 10^5 M^{-1} ($K_{D,app}$ = 4.1 ± 1.4 μM), a heat of binding of ΔH_{app} = -17.3 ± 0.1 kcal/mol and with an average binding stoichiometry of z = 65.1 ± 0.1 lipids per protein molecule (Table 8). The membrane binding analysis suggests annexin a5 has greater affinity for cholesterol containing membrane in the presence of calcium ion as opposed to membrane without cholesterol.

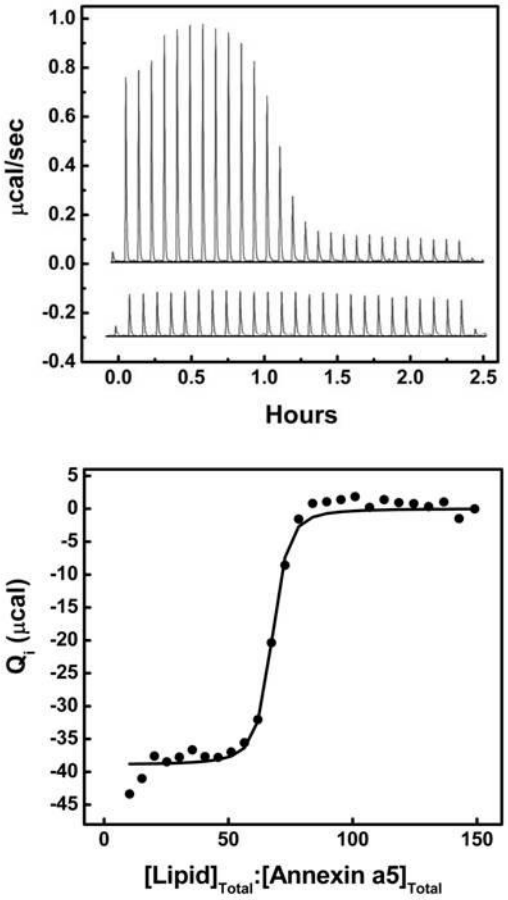

Figure 6.6: Results of the titration of 30 μM annexin a5 with lipid as LUVs made of a (60:40):10 mixture of (POPC:POPS):Chol in the presence of 0.75 mM Ca^{2+} at 15°C. *Top*: Raw ITC data. *Bottom*: Integrated heats of binding as a function of ligand to protein ratio.

TABLE 8: Thermodynamic parameters of compositions of (60:40):5 and (60:40):10 (POPC:POPS):Chol membrane binding of annexin a5 in the presence of calcium

	Membrane Binding with Saturating Ca^{2+} Present		
	60:40 POPC:POPS	(60:40):5 (POPC:POPS):Chol	(60:40):10 (POPC:POPS):Chol
N	z = 46.5 ± 0.1	z = 57.0 ± 0.4	z = 65.1 ± 0.1
K (M^{-1})	78000 ± 4000	192000 ± 61000	242000 ± 69000
K_D (μM)	13 ± 1.0	5.2 ± 2.0	4.1 ± 1.4
ΔH (kcal/mol)	-17.3 ± 0.1	-20.0 ± 0.1	-17.3 ± 0.1
$T\Delta S$ (kcal/mol)	-10.9 ± 0.1	-13.1 ± 0.2	-10.2 ± 0.2
ΔG (kcal/mol)	-6.4 ± 0.1	-6.9 ± 0.2	-7.1 ± 0.2

*Reported error represents 95% confidence intervals. Cholesterol containing membrane binding in the presence of saturating calcium is compared to that of non-cholesterol containing membrane binding.

6.2 DISCUSSION

The combined Ca^{2+} and membrane binding data presented suggests that annexin a5's calcium and membrane binding affinity is modified with the addition of cholesterol. Moreover, the total number of solution state calcium binding sites is no longer conserved in the presence of cholesterol containing membrane. Thus, the membrane composition seems to be modulating the protein's binding response in the presence of calcium ion. These changes in binding profiles upon addition of cholesterol (shown in Figures 6.1-6.6) could possibly allude to the diverse functionality of the annexins and more specifically, help clarify the role of annexin a5 in membrane repair.

CONCLUSIONS

The ITC results presented here suggest membrane organization and composition modulates the binding affinity of annexin a5. In the presence of both non-cholesterol and cholesterol containing membrane, annexin a5's affinity for calcium ion is greatly enhanced. Moreover, upon incorporation of the physiologically relevant lipid, cholesterol, the presence of additional calcium binding sites suggests a conformational change in the protein allowing calcium sequestering in solution. These data are consistent with the observation that annexin a5 has the ability to bind between 5 and 12 calcium ions in solution [82]. The cooperative binding response shown in the presence of both membrane compositions suggests a means for signal propagation involving a combination of protein-lipid and lipid-lipid interactions on the membrane surface. Furthermore, the distinct differences in binding profiles in the presence of varying membrane compositions and calcium ion suggest a diverse functional role of annexin a5 in membrane repair.

REFERENCES:

1. Shimshick, E.J. and H.M. McConnell, *Lateral phase separation in phospholipid membranes.* Biochemistry, 1973. **12**(12): p. 2351-2360.
2. Karnovsky, M.J., et al., *The concept of lipid domains in membranes.* Journal of Cell Biology, 1982. **94**(1): p. 1-6.
3. Simons, K. and D. Toomre, *Lipid rafts and signal transduction.* Nature Reviews. Molecular Cell Biology., 2000. **1**(1): p. 31-39.
4. Honerkamp-Smith, A.R., S.L. Veatch, and S.L. Keller, *An introduction to critical points for biophysicists; observations of comopositional heterogeneity in lipid membranes.* Biochemica et Biophysica Acta, 2009. **1788**(1): p. 53-63.
5. Veatch, S.L., et al., *Critical fluctuations in plasma membrane vesicles.* ACS Chemical Biology, 2008.
6. Brown, D.A. and E. London, *Functions of lipid rafts in biological membranes.* Annual review of cell and developmental biology, 1998. **14**: p. 111-136.
7. Baird, B., E.D. Sheets, and D. Holowka, *How does the plasma membrane participate in cellular signaling by receptors for immunoglobulin E?* Biophysical Chemistry, 1999. **82**(2-3): p. 109-119.
8. Tanford, C., *The hydrophobic effect and the organization of living matter.* Science, 1978. **200**(4345): p. 1012-1018.
9. Gennis, R.B., *Biomembranes: Molecular Structure and Function*. First Edition ed. Biomembranes: Molecular Structure and Function, ed. C.R. Cantor. 1989, New York, NY: Springer-Verlag. 533.
10. Ipsen, J.H., et al., *Phase equilibria in the phosphatidylcholine-cholesterol system.* Biochemica et Biophysica Acta, 1987. **905**(1): p. 162-172.
11. Recktenwald, D.J. and H.M. McConnell, *Phase equilibria in binary mixtures of phosphatidylcholine and cholesterol.* Biochemistry, 1981. **20**(15): p. 4505-4510.
12. Copeland, B.R. and H.M. McConnell, *The rippled structure in bilayer membranes of phosphatidylcholine and binary mixtures of phosphatidylcholine and cholesterol.* Biochemica et Biophysica Acta, 1980. **559**(1): p. 95-109.
13. Vist, M.R. and J.H. Davis, *Phase equilibria of cholesterol/dipalmitoylphosphatidylcholine mixtures: 2H nuclear magnetic resonsance and differential scanning calorimetry.* Biochemistry, 1990. **29**(2): p. 451-464.
14. Singer, S.J. and G.L. Nicolson, *The fluid mosaic model of the structure of cell membranes.* Science, 1972. **175**(4023): p. 720-731.
15. Lee, A.G., et al., *Clusters in lipid bilayers and the interpretation of thermal effects in biological membranes.* Biochemistry, 1974. **13**(18): p. 3699-3705.
16. Hinderliter, A.K., J. Huang, and G.W. Feigenson, *Detection of phase separation in fluid phosphatidylserine/phosphatidylcholine mixtures.* Biophysical Journal, 1994. **67**(5): p. 1906-1911.
17. Feigenson, G.W., *Phase diagrams and lipid domains in multicomponent lipid bilayer mixtures.* Biochemica et Biophysica Acta, 2009. **1788**(1): p. 47-52.
18. Veatch, S.L. and S.L. Keller, *Miscibility phase diagrams of giant vesicles containing sphingomyelin.* Physical Review Letters, 2005. **94**(148101): p. 1-4.

19. Frazier, M.L., et al., *Investigation of domain formation in sphingomyelin/cholesterol/POPC mixtures by fluorescence resonance energy transfer and Monte Carlo simulations.* Biophysical Journal, 2007. **92**(7): p. 2422-2433.
20. Almeida, P.F.F., *Thermodynamics of lipid interactions in complex bilayers.* Biochemica et Biophysica Acta, 2009. **1788**(1): p. 72-85.
21. Almeida, P.F., W.L. Vaz, and T.E. Thompson, *Percolation and diffusion in three-component lipid bilayers: effect of cholesterol on an equimolar mixture of two phosphatidylcholines.* Biophysical Journal, 1993. **64**(2): p. 339-412.
22. Almeida, P.F.F., A. Pokorny, and A. Hinderliter, *Thermodynamics of membrane domains.* Biochemica et Biophysica Acta, 2005. **1720**(1-2): p. 1-13.
23. Xu, X. and E. London, *The effect of sterol structure of membrane lipid domains reveals how cholesterol can induce lipid domain formation.* Biochemistry, 2000. **39**(5): p. 844-849.
24. Wang, J., Megha, and E. London, *Relationship between sterol/steroid structure and participation in ordered lipid domains(lpid rafts): implications for lipid raft structure and function.* Biochemistry, 2004. **43**(4): p. 1010-1018.
25. Silvius, J.R., *Role of cholesterol in lipid raft formation: lessons from lipid model systems.* Biochemica et Biophysica Acta, 2003. **1610**(2): p. 174-183.
26. Field, K.A., D. Holowka, and B. Baird, *Fc epsilon RI-mediated recruitment of p53/56lyn to detergent-resistant membrane domains accompanies cellular signaling.* Proceedings of the National Academy of Sciences of the United States of America, 1995. **92**(20): p. 9201-9205.
27. Brown, D.A. and J.K. Rose, *Sorting of GPI-anchored proteins to glycolipid-enriched membrane subdomains during transport to the apical cell surface.* Cell, 1992. **68**(3): p. 533-544.
28. Simons, K. and G. van Meer, *Lipid sorting in epithelial cells.* Biochemistry, 1988. **27**(17): p. 6197-6202.
29. Pike, L.J., *The challenge of lipid rafts.* Journal of Lipid Research, 2009(April Supplement): p. 323-328.
30. Sheets, E.D., D. Holowka, and B. Baird, *Membrane organization in immunoglobulin E receptor signaling.* Current Opinion in Chemical Biology, 1999. **3**(1): p. 95-99.
31. Veatch, S.L. and S.L. Keller, *Seeing spots: complex phase behavior in simple membranes.* Biochemica et Biophysica Acta, 2005. **1746**(3): p. 172-185.
32. Zhao, J., et al., *Phase studies of model biomembranes: complex behavior of DSPC/DOPC/cholesterol.* Biochemica et Biophysica Acta, 2007. **1768**(11): p. 2764-2776.
33. Miao, L., et al., *From lanosterol to cholesterol: structural evolution and differential effects on lipid bilayers.* Biophysical Journal, 2002. **82**(3): p. 1429-1444.
34. Sankaram, M.B. and T.E. Thompson, *Cholesterol-induced fluid-phase immiscibility in membranes.* Proceedings of the National Academy of Sciences, 1991. **88**(19): p. 8686-8690.

35. Sankaram, M.B. and T.E. Thompson, *Modulation of phospholipid acyl chain order by cholesterol. A solid-state ^2H nuclear magnetic resonance structure.* Biochemistry, 1990. **29**(47): p. 10676-10684.
36. Brown, D.A. and E. London, *Structure and origin of ordered lipid domains in biological membranes.* Journal of Membrane Biology, 1998. **164**(2): p. 103-114.
37. Kuzmin, P.I., et al., *Line tension and interaction energies of membrane rafts calculated from lipid splay and tilt.* Biophysical Journal, 2005. **88**(2): p. 1120-1133.
38. Lawrence, J.C., et al., *Real-time analysis of the effects of cholesterol on lipid raft behavior using atomic force microscopy.* Biophysical Journal, 2003. **84**(3): p. 1827-1832.
39. Yuan, C., et al., *The size of lipid rafts: an atomic force microscopy study of ganglioside GM1 domains in sphingomyelin/DOPC/cholesterol membranes.* Biophysical Journal, 2002. **82**(5): p. 2526-2535.
40. Gandhavadi, M., et al., *Structure, composition, and peptide binding properties of detergent soluble bilayers and detergent resistant rafts.* Biophysical Journal, 2002. **82**(3): p. 1469-1482.
41. Garcia-Saez, A.J., S. Chiantia, and P. Schwille, *Effect of line tension on the lateral organization of lipid membranes.* Journal of Biological Chemistry, 2007. **282**(46): p. 33537-33544.
42. Nicolini, C., et al., *Visualizing association of N-ras in lipid microdomains: influence of domain structure and interfacial adsorption.* Journal of the American Chemical Society, 2006. **128**(1): p. 192-201.
43. Morgan, R.O. and M.P. Fernández, *Molecular phylogeny of annexins and identification of a primitive homologue in Giardia lamblia.* Molecular Biology and Evolution, 1995. **12**(6): p. 967-979.
44. Gerke, V. and S.E. Moss, *Annexins: from structure to function.* Physiological Reviews, 2002. **82**(2): p. 331-371.
45. Creutz, C.E., C.J. Pazoles, and H.B. Pollard, *Identification and purification of an adrenal medullary protein (synexin) that causes calcium-dependent aggregation of isolated chromaffin granules.* Journal of Biological Chemistry, 1978. **253**(8): p. 2858-2866.
46. Geisow, M.J., et al., *A consensus amino-acid sequence repeat in Torpedo and mammalian Ca^{2+}-dependent membrane-binding proteins.* Nature 1986. **320**(6063): p. 636-638.
47. Concha, N.O., et al., *Rat annexin V crystal structure: Ca^{2+}-induced conformational changes.* Science, 1993. **261**(5126): p. 1321-1324.
48. Huber, R., J. Römisch, and E.P. Paques, *The crystal and molecular structure of human annexin V, an anticoagulant protein that binds to calcium and membranes.* EMBO Journal, 1990. **9**(12): p. 3867-3874.
49. Swairjo, M.A. and B.A. Seaton, *Annexin structure and membrane interactions: a molecular perspective.* Annual Review of Biophysics and Biomolecular Structure, 1994. **23**: p. 193-213.

50. Draeger, A., K. Monastyrskaya, and E.B. Babiychuk, *Plasma membrane repair and cellular damage control: The annexin survival kit.* Biochemical Pharmacology, 2011. **81**(6): p. 703-712.
51. Moss, S.E. and R.O. Morgan, *The annexins.* Genome Biology, 2004. **5**(4): p. 219.
52. Lewit-Bentley, A., et al., *The effect of metal binding on the structure of annexin V and implications for membrane binding.* European Journal of Biochemistry, 1992. **210**(1): p. 73-77.
53. Rosengarth, A., et al., *Folding energetics of ligand binding proteins II. Cooperative binding of Ca^{2+} to annexin I.* Journal of Molecular Biology, 2001. **306**(4): p. 825-835.
54. Campos, B., et al., *Mutational and crystallographic analyses of interfacial residues in annexin V suggest direct interactions with phospholipid membrane components.* Biochemistry, 1998. **37**(22): p. 8004-8010.
55. Almeida, P.F., et al., *Allosterism in membrane binding: a common motif of the annexins?* Biochemistry, 2005. **44**(32): p. 10905-10913.
56. Tait, J.F., D.F. Gibson, and C. Smith, *Measurement of the affinity and cooperativity of annexin V-membrane binding under conditions of low membrane occupancy.* Analytical Biochemistry, 2004. **329**(1): p. 112-119.
57. Schlaepfer, D.D., et al., *Structural and functional characterization of endonexin II, a calcium-and phospholipid-binding protein.* Proceedings of the National Academy of Sciences of the United States of America, 1987. **84**(17): p. 6078-6082.
58. Ernst, J.D., A. Mall, and G. Chew, *Annexins possess functionally distinguishable Ca^{2+} and phospholipid binding domains.* Biochemical and Biophysical Research Communications, 1994. **200**(2): p. 867-876.
59. Vats, K., et al., *Peripheral protein organization and its influence on lipid diffusion in biomimetic membranes.* ACS Chemical Biology, 2010. **5**(4): p. 393-403.
60. Concha, N.O., et al., *Annexin V forms calcium-dependent trimeric units on phospholipid vesicles.* FEBS Letters, 1992. **314**(2): p. 159-162.
61. Pigault, C., et al., *Formation of two-dimensional arrays of annexin V on phosphatidylserine-containing liposomes.* Journal of Molecular Biology, 1994. **236**(1): p. 199-208.
62. Oling, F., W. Bergsman-Schutter, and A. Brisson, *Trimers, dimers of trimers, and trimers of trimers are common building blocks of annexin a5 two-dimensional crystals.* Journal of Structural Biology, 2001. **133**(1): p. 55-63.
63. van Meer, G. and K. Simons, *Lipid polarity and sorting in epithelial cells.* Journal of Cellular Biochemistry, 1988. **36**(1): p. 51-58.
64. van Dijck, P.W., *Negatively charged phospholipids and their position in the cholesterol affinity sequence.* Biochemica et Biophysica Acta, 1979. **555**(1): p. 89-101.
65. Stamatotos, L. and J.R. Silvius, *Effects of cholesterol on the divalent cation-mediated interactions of vesicles containing amino and choline phospholipids.* Biochemica et Biophysica Acta, 1987. **905**(1): p. 81-90.

66. Almeida, P.F., A. Best, and A. Hinderliter, *Monte Carlo simulation of protein-induced lipid demixing in a membrane with interactions derived from experiment.* Biophysical Journal, 2011. **101**(8): p. 1930-1937.
67. Drust, D.S. and C.E. Creutz, *Aggregation of chromaffin granules by calpactin at micromolar levels of calcium.* Nature, 1988. **331**(6151): p. 88-91.
68. *Avanti Polar Lipids*. 2010 [cited 2010 October 2010]; Available from: http://avantilipids.com/.
69. Knutson, K.J., *The thermodynamic basis for the binding of lipids to annexin a5.*, in *Chemistry and Biochemistry*. 2009, University of Minnesota Duluth: Duluth. p. 41.
70. Tsien, R.Y., *New calcium indicators and buffers with high selectivity against magnesium and protons: design, synthesis, and properties of prototype structures.* Biochemistry, 1980. **19**(11): p. 2396-2404.
71. Kingsley, P.B. and G.W. Feigenson, *The synthesis of a perdeuterated phospholipid: 1,2-dimyristoyl-sn-glycero-3-phospholcholine-d72.* Chemistry and Physics of Lipids, 1979. **24**(2): p. 135-147.
72. Berg, J.M., J.L. Tymoczko, and L. Stryer, *Biochemistry*. Sixth ed, ed. S. Moran. 2007, New York, NY: W. H. Freeman and Company. 1026.
73. Zaks, W.J. and C.E. Creutz, *Ca^{2+}-dependent annexin self-association on membrane surfaces.* Biochemistry, 1991. **30**(40): p. 9607-9615.
74. *User's Manual Model CSC 5300 Nano-Isothermal Titration Calorimeter III*, C.S. Corporation, Editor. 2005, Calorimetry Sciences Corporation: Lindon, Utah. p. 69.
75. Wiseman, T., et al., *Rapid measurement of binding constants and heats of binding using a new titration calorimeter.* Analytical Biochemistry, 1989. **179**(1): p. 131-137.
76. *ITC Data Analysis in Origin: Tutorial Guide*, MicroCal, Editor. 1998. p. 81.
77. Wyman, J. and S.J. Gill, *Binding and Linkage: Functional Chemistry of Biological Molecules*. 1990, Mill Valley, CA: University Science Books. 330.
78. Dill, K.A. and S. Bromberg, *Molecular driving forces: statistical thermodynamics in biology, chemistry, physics, and nanoscience.* Second Edition ed. 2011, New York, NY: Garland Science, Taylor & Francis Group, LLC. 756.
79. Wiseman, T., et al., *Rapid measurement of binding constants and heats of binding using a new titration calorimeter.* Anal. Biochem., 1989. **179**(1): p. 131-137.
80. Monod, J., J. Wyman, and J.P. Changeux, *On the nature of allosteric transitions: a plausible model.* Journal of Molecular Biology, 1965. **12**: p. 88-118.
81. Kenakin, T., *Allosteric theory: taking therapeutic advantage of the malleable nature of GPCRs.* Current Neuropharmacology, 2007. **5**(3): p. 149-156.
82. Jin, M., et al., *Essential role of B-helix calcium binding sites in annexin V-membrane binding.* Journal of Biological Chemistry, 2004. **279**(39): p. 40351-40357.